Beyond the carapace: skull shape variation and morphological systematics of long-nosed armadillos (genus *Dasypus*)

Lionel Hautier [Corresp., 1, 2] , Guillaume Billet [3] , Benoit De Thoisy [4, 5] , Frédéric Delsuc [6]

1 Institut des Sciences de l'Evolution, UMR5554, CNRS, IRD, EPHE, Université de Montpellier, Montpellier, France

2 Mammal Section, Life Sciences, Vertebrate Division, The Natural History Museum, London, United Kingdom

3 Museum National d'Histoire Naturelle, CR2P, UMR 7207, CNRS, Université Paris 6, Paris, France

4 Institut Pasteur de la Guyane, Cayenne, France

5 Kwata NGO, Cayenne, France

6 Institut des Sciences de l'Evolution, UMR 5554, CNRS, IRD, EPHE, Université de Montpellier, Montpellier, France

Corresponding Author: Lionel Hautier
Email address: lionel.hautier@umontpellier.fr

Background. The systematics of long-nosed armadillos (genus *Dasypus*) has been mainly based on a handful of external morphological characters and classical measurements. Here, we studied the pattern of morphological variation in the skull of long-nosed armadillos species, with a focus on the systematics of the widely distributed nine-banded armadillo (*D. novemcinctu*s). **Methods.** We present the first exhaustive 3D comparison of the skull morphology within the genus *Dasypus*, based on µCT-scans. We used geometric morphometric approaches to explore the patterns of the intra- and interspecific morphological variation of the skull with regard to several factors such as taxonomy, geography, allometry, and sexual dimorphism. **Results.** We show that the shape and size of the skull vary greatly among *Dasypus* species, with *D. pilosus* representing a clear outlier compared to other long-nosed armadillos. The study of the cranial intraspecific variation in *D. novemcinctus* evidences clear links to the geographic distribution and argues in favour of a revision of past taxonomic delimitations. Our detailed morphometric comparisons detected previously overlooked morphotypes of nine-banded armadillos, especially a very distinctive unit restricted to the Guiana Shield. **Discussion.** As our results are congruent with recent molecular data and analyses of the structure of paranasal sinuses, we propose that *D. novemcinctus* should be regarded either as a polytypic species (with three to four subspecies) or as a complex of several distinct species.

1 **Beyond the carapace: skull shape variation and morphological systematics of**

2 **long-nosed armadillos (genus *Dasypus*).**

4 Lionel Hautier[1,2], Guillaume Billet[3], Benoit de Thoisy[4,5], and Frédéric Delsuc[1]

6 [1]Institut des Sciences de l'Evolution, UMR5554, CNRS, IRD, EPHE, Université de Montpellier,

7 Montpellier, France.

8 [2]Mammal Section, Life Sciences, Vertebrate Division, The Natural History Museum, London,

9 UK.

10 [3]Sorbonne Universités, CR2P, UMR 7207, CNRS, Université Paris 6, Muséum National

11 d'Histoire Naturelle, Paris, France.

12 [4]Institut Pasteur de la Guyane, Cayenne, France.

13 [5]Kwata NGO, Cayenne, France.

16 **Corresponding Author**

17 Lionel Hautier

18 Email address: lionel.hautier@umontpellier.fr.

Abstract

Background. The systematics of long-nosed armadillos (genus *Dasypus*) has been mainly based on a handful of external morphological characters and classical measurements. Here, we studied the pattern of morphological variation in the skull of long-nosed armadillos species, with a focus on the systematics of the widely distributed nine-banded armadillo (*D. novemcinctu*s).

Methods. We present the first exhaustive 3D comparison of the skull morphology within the genus *Dasypus*, based on µCT-scans. We used geometric morphometric approaches to explore the patterns of the intra- and interspecific morphological variation of the skull with regard to several factors such as taxonomy, geography, allometry, and sexual dimorphism.

Results. We show that the shape and size of the skull vary greatly among *Dasypus* species, with *D. pilosus* representing a clear outlier compared to other long-nosed armadillos. The study of the cranial intraspecific variation in *D. novemcinctus* evidences clear links to the geographic distribution and argues in favour of a revision of past taxonomic delimitations. Our detailed morphometric comparisons detected previously overlooked morphotypes of nine-banded armadillos, especially a very distinctive unit restricted to the Guiana Shield.

Discussion. As our results are congruent with recent molecular data and analyses of the structure of paranasal sinuses, we propose that *D. novemcinctus* should be regarded either as a polytypic species (with three to four subspecies) or as a complex of several distinct species.

Introduction

With their Pan-American distribution, long-nosed armadillos (genus *Dasypus*) constitute an understudied model for Neotropical biogeography. They are the most taxonomically diverse and widespread extant xenarthrans. The genus *Dasypus* traditionally comprises seven extant species (*D. novemcinctus*, *D. hybridus*, *D. septemcinctus*, *D. kappleri*, *D. pilosus*, *D. mazzai*, and *D. sabanicola*; Wetzel, 1985; Wilson & Reeder, 2005; Feijo & Cordeiro-Estrela, 2014) and two extinct ones (*D. bellus* and *D. punctatus*; Castro et al., 2013; Castro, 2015). In spite of being one of the earliest diverging cingulate lineages (Gaudin & Wible, 2006; Delsuc et al., 2012; Gibb et al., 2016), the early evolutionary history of dasypodines remains poorly known (Castro, 2015). Only three extinct genera are currently recognized among the Dasypodini: *Anadasypus* from the middle Miocene of Colombia and late Miocene of Ecuador (Carlini, Vizcaíno & Scillato-yané, 1997; Carlini et al., 2013), *Pliodasypus* from the late Pliocene of Venezuela (Castro et al., 2014), and *Propraopus* from the middle Pleistocene–early Holocene of South America (Castro et al., 2013a).

Aside from the widespread nine-banded armadillo (*D. novemcinctus*), all extant long-nosed armadillos are restricted to South America. Some species are sympatric in certain areas, resulting in competition and possibly supporting divergent behaviours and morphologies. The nine-banded armadillo is likely to be the most abundant armadillo in tropical forests (Wetzel & Mondolfi, 1979; Loughry & McDonough, 1998), and it has the widest distribution of all extant xenarthran species. Its distribution is thought to cover much of South and Central America and parts of North America, and it ranges from the southeastern United States to northwestern Argentina and Uruguay (McBee & Baker, 1982; Loughry & McDonough, 2013). The species ability to disperse quickly, as well as its opportunistic and generalist mode of life, could partly

60   explain this broad distribution (Smith & Doughty, 1984; Loughry & McDonough, 1998, 2013) as

61   well as its rapid historical expansion into the United States (Taulman & Robbins, 2014). Such a

62   wide geographical distribution, combined with long-recognized morphological variations (Peters,

63   1864; Gray, 1873; Allen, 1911; Lönnberg, 1913; Russell, 1953), raise the possibility that major

64   taxonomic subgroups have been overlooked, be it at the subspecific or even specific level.

65   As its vernacular name implies, the genus *Dasypus* is characterized by a long, slender

66   rostrum, which represents at least 55% of the length of the head (Gardner, 2008). The different

67   species are usually distinguished by body and cranial measurements, colour differences, and

68   morphological features of the carapace, such as the number of movable bands and scutes across

69   the body and the number and shape of osteodermal foramina (Wetzel, 1985; Feijo & Cordeiro-

70   Estrela, 2016). The carapace is a hallmark of armadillos, and constitutes such a unique feature

71   for mammals that it has dominated the attention of early and modern anatomists and, as a result,

72   partly jeopardized the classification of the group. Its morphology, chiefly the number of movable

73   bands, has been extensively used in systematic studies. However, even in the so-called nine-

74   banded armadillo, the number of movable bands can vary from 7 to 11 (Wetzel & Mondolfi, 1979;

75   McBee & Baker, 1982). Yet early on, in his Systema Naturae, Linnaeus (1758:51) cast doubt on

76   the usefulness of the number of movable bands as a criterion to distinguish *Dasypus* species (in

77   this case *D. septemcinctus* from *D. novemcinctus*). Since then, a number of authors have raised

78   the question whether such external features could be confidently used for systematic purposes.

79   Wetzel and Mondolfi (1979:46) argued that "although many scientific names of armadillos are

80   based on the number of movable bands, it is proposed here that for vernacular names we

81   discontinue using this variable characteristic and base names upon unique or more consistent

82   features." In the early 20th century, Hamlett (1939) made similar observations on the nine-banded

83   armadillo. He considered it impossible to recognize external variations at a subspecific level, and

84   concluded that "cranial characters appear to offer the only promise for subspecific analysis of the

85   species" (Hamlett 1939:335). We decided to further investigate Hamlett's idea, since no large

86   review of the dasypodine cranial variation has been undertaken to date.

87   This study aims to further elucidate the pattern of morphological variation seen in the

88   skull of long-nosed armadillos, with a focus on the nine-banded armadillo. Geometric

89   morphometric data were collected for most *Dasypus* species using μCT-scans. The main

90   questions asked in the present study are whether different patterns of variation in skull shape can

91   be characterized among and within long-nosed armadillo species, and if those patterns could be

92   linked to factors such as taxonomy, geographical distribution, skull size, or sexual dimorphism.

93   Our ultimate goals are to reconstruct the details of the biogeographic distribution of the

94   widespread nine-banded armadillo at the continental scale and to lay the path for a new

95   integrative taxonomy of long-nosed armadillos. A greater understanding of the morphological

96   diversity and patterns of evolution for long-nosed armadillos is timely to effectively conserve

97   these species, and will also serve to deepen our knowledge of their peculiar evolution and

98   biology (Loughry & McDonough, 2013).

99

100   **Materials & Methods**

101   ***Biological samples***

102   The material studied came from the collections of the Muséum national d'Histoire naturelle

103   (MNHN, collections Zoologie et Anatomie comparée, Mammifères et Oiseaux) in Paris (France),

104   the Natural History Museum (BMNH) in London (UK), the Naturalis Biodiversity Center (NBC)

105   in Leiden (Holland), the Royal Ontario Museum (ROM) in Toronto (Canada), the Museum of

106   Natural Science of the Louisiana State University (LSU) in Bâton-Rouge (USA), the American

107   Museum of Natural History (AMNH) in New York (USA), the National Museum of Natural

108   History (NMNH) in Washington (USA), the Instituto de Pesquisas Científicas e Tecnológicas do

109   Estado do Amapá (IEPA) in Macapá (Brazil), and the Muséum d'Histoire Naturelle in Geneva

110   (Switzerland), the KWATA association in Cayenne (French Guiana), and the personal collection

111   of Pierre Charles-Dominique in Montpellier (France). We analysed 128 skulls belonging to five

112   *Dasypus* species (see Table S1 for a complete list of specimens): *D. novemcinctus*, *D. hybridus*,

113   *D. septemcinctus*, *D. kappleri*, and *D. pilosus* (no data was available for *D. mazzai*, and *D.*

114   *sabanicola*). With these data we performed a preliminary assessment of the average amounts of

115   cranial variation at the specific level among different populations of *D. novemcinctus* from

116   French Guiana, Guyana, Suriname, Ecuador, Brazil, Venezuela, Colombia, Costa Rica, Belize,

117   Bolivia, Argentina, Paraguay, Uruguay, Panama, Nicaragua, Honduras, Guatemala, Mexico,

118   Peru, and the USA (Table S1). Juvenile, subadult, and adult specimens were considered in order

119   to take into account the effect of age, size, and differential growth on the dataset. Several studies

120   (Hensel, 1872; Russell, 1953; Ciancio et al., 2012) showed that long-nosed armadillos possess

121   tooth replacement, as is typical for mammals, and that the eruption of permanent teeth occurs

122   relatively late, as observed in afrotherians (Asher & Lehmann, 2008). Accordingly, we used

123   eruption of the teeth, suture closure, and size (i.e., skull length) as criteria to identify adult

124   specimens in our dataset. Specimens were considered as juveniles when they displayed milk

125   teeth and an open suture between the basioccipital and the basisphenoid. Subadults were

126   characterized by erupting permanent teeth. Adult specimens always showed a closed

127   basioccipital/basisphenoid suture and a fully erupted permanent dentition. Except when

128   specified, only adults and subadults specimens were considered in the morphometrical analyses.

129

130   ***Geometric morphometric methods***

131   Due to the limitations of the classical qualitative descriptive approach, geometric morphometrics

132   represents a good complementary technique by which to examine intraspecific shape variation.

133   Digital data for all specimens were acquired using X-ray micro-computed tomography (µCT) at

134   the University of Montpellier (France), at the Natural History Museum (London, UK), and at the

135   AST-RX platform MNHN (Paris, France). Three-dimensional reconstruction and visualization of

136   the skulls were performed using stacks of digital µCT images with AVIZO v. 6.1.1 software

137   (Visualization Sciences Group 2009). The mandibles and crania of armadillos were quantified

138   with 10 and 84 anatomical landmarks respectively (Fig. 1 and Tables 1 and 2) using ISE-

139   MeshTools (version 1.3.1; Lebrun, 2014). These landmarks were inspired by previous studies

140   performed on different mammalian taxa (Hautier, Lebrun & Cox, 2012; Hautier et al., 2014).

141   Considering the tendency toward the reduction of the number of teeth in *Dasypus* (Allen, 1911),

142   specimens often lack the last dental locus, which corresponds to a molar (Ciancio et al., 2012). In

143   order to avoid producing an artificial shortening of the entire tooth row, we decided not to place

144   a landmark at the end of the tooth row, as it is commonly the case, but after the last premolar

145   locus (in both mandible and maxilla). Since skulls were often incomplete, the number of

146   landmarks was adjusted to incorporate the maximal morphological variation in a maximum

147   number of individuals. This number differed when we performed analyses including all *Dasypus*

148   species (10 and 70 landmarks for the mandible and the cranium respectively) or only *D.*

149   *novemcinctus* (10 and 82 landmarks for the mandible and the cranium respectively).

150   All configurations (sets of landmarks) were superimposed using the Procrustes method of

151   generalized leastsquares superimposition (GLS scaled, translated, and rotated configurations so

152   that the intralandmark distances were minimized) following the methods of Rohlf (1999) and

153   Bookstein (1991). Subsequently, mandibular and cranial forms of each specimen were

154   represented by centroid size S, and by multidimensional shape vector v in linearized Procrustes

155   shape space. Shape variability of the skull and the mandible was analysed by Principal

156   Component Analysis (PCA) of shape (Dryden & Mardia, 1998). Analysis and visualization of

157   patterns of shape variation were performed with the interactive software package

158   MORPHOTOOLS (Specht, 2007; Specht, Lebrun & Zollikofer, 2007; Lebrun, 2008; Lebrun et

159   al., 2010).

160   To account for the potentially confounding effects of size allometry on shape of the

161   cranium and mandible at the intraspecific level (i.e., within *D. novemcinctus*), size-corrected

162   shapes were obtained as follows: we conducted a multivariate regression of Procrustes residuals

163   on the logarithm of the centroid size, yielding an allometric shape vector (ASV). The allometric

164   shape vector represents a direction in shape space, which characterizes mandibular and cranial

165   allometric patterns. All crania and mandibles of *D. novemcinctus* were then projected on

166   allometric shape vectors, the residuals representing the component of skull shape that is

167   independent of size. Shape variation independent of size was analyzed by PCA of shape using

168   MORPHOTOOLS. PCres corresponds to principal components of a PCA performed on shape

169   data corrected for allometry. The same analyses could not be performed at the interspecific level

170   due to large differences in sample size.

171   Multivariate analyses of variance (MANOVA) were performed on the principal component

172   scores of mandibular and cranial mean shapes in order to assess the effects of different factors on

173   mandibular and cranial shape variation: clades (species), sex, and geographic distribution

174   (countries). Because our dataset consisted of a relatively large number of variables, the shape

175   space was simplified to the first Principal Components (the number of PCs was defined in order

176   to keep 90% of the interspecific shape variance). Manovas were performed with Past 2.06

177   (Hammer, Harper & Ryan, 2001). Linear discriminant analyses (LDA) of shape coordinates were

178   performed on the same number of PCs to assess a potential discrimination of skull morphology

179   in relation to phylogeny (*i.e.*, species) and geography (*i.e.*, countries). If lumping specimens by

180   country has little biological relevance, we consider that using such artificial boundaries also

181   constitutes a mean to avoid making *a priori* hypotheses. In all cases, all LDA results were

182   double-checked with post hoc classification methods and PCA results. When a group included

183   only one individual, this specimen was integrated into the dataset as an ungrouped case. A skull

184   from Panama (NMNH 171052) was not complete enough to be considered in these analyses. We

185   then decided to perform similar analyses with a reduced set of landmarks (81 landmarks on the

186   cranium) to enable its morphological comparison with other specimens.

187

188   ***Linear measurements***

189   Several linear measurements of the skull of *Dasypus* were calculated directly on 3D coordinates

190   of landmarks (Fig. 2). These measurements were used to compare our results with traditional

191   methods of species delineation.

192

193   **Results**

194   ***Interspecific variation of skull shape among long-nosed armadillos***

195   A Manova performed on the first 35 PCs (i.e. 90% of the variance) indicates a significant

196   morphological differentiation of the mandibles and crania relative to species delimitations

197   (mandible Wilks' lambda=0.01164, F=4.903, p<0.001; cranium Wilks' lambda=0.0005897,

198   F=11, p<0.001). A multivariate regression of the shape component on size, estimated by the

199   logarithm of centroid size, was significant for the skull (mandible Wilks' lambda=0.2709,

200   F=6.637, p<0.001; cranium Wilks' lambda=0.0632, F=30.92, p<0.001).

201   Morphological differences occur among the mandibles of the five species of *Dasypus*

202   (Fig. 3A). The first two principal components (24.73% and 16.48% of total shape variation)

203   weakly discriminates *D. pilosus* (negative values) from *D. kappleri* (positive values) while all

204   specimens of *D. novemcinctus*, *D. hybridus*, and *D. septemcinctus* sit in the middle of the graph.

205   These axes separate mandibles having a slender horizontal ramus, an elongated anterior part

206   (located in front of the tooth row), a short ascending ramus, and a short, anteriorly positioned and

207   vertically oriented coronoid process, from mandibles showing a high horizontal ramus, a short

208   anterior region, a long ascending ramus, and an elongated and distally oriented coronoid process.

209   Mandibles of different size are poorly discriminated along the first principal component (Fig.

210   3B).

211   The interspecific differences in the cranium of *Dasypus* are apparent in the morphospace

212   defined by the first two principal components. Except for *D. hybridus* and *D. septemcinctus*, all

213   species are well discriminated in the morphospace defined by the two first principal components

214   (Fig. 4A), which explain 28.76% and 15.29% of the variance respectively. The first principal

215   component unequivocally discriminates *D. hybridus* and *D. septemcinctus* from other species,

216   and negatively correlates with a shortened rostrum and enlarged basicranium and braincase (Fig.

217   4A). *D. pilosus* individuals are well discriminated on the second principal component. On PC2

218   (Fig. 4A), the crania of *D. pilosus* appear narrower, with a long snout and smaller braincase

219   (positive values), whereas the crania of *D. novemcinctus*, *D. kappleri*, *D. hybridus*, and *D.*

220   *septemcinctus* are wider, with a shorter snout and relatively small braincase (negative values). A

221 regression of the first principal component on the logarithm of the centroid size (Fig. 4B) clearly

222 shows that the five species show different size ranges. The biggest crania are long and display a

223 longer and wider snout, whereas the smallest crania are short and wide posteriorly and

224 characterized by a short snout. *A posteriori* classification methods produced 100% correct

225 specific classification of specimens.

226   We also performed the same analyses, this time including juvenile specimens (Figure S2)

227 but excluding *D. pilosus*, since it represents a clear outlier in the morphospace. All juvenile

228 specimens of *D. novemcinctus* tend to exhibit negative values for PC1, and thus appear more

229 similar in shape to *D. septemcinctus* and *D. hybridus* than the adult *D. novemcinctus*. All

230 juveniles of *D. novemcinctus* and *D. septemcinctus* exhibit more negative values of PC1 and

231 more positive values of PC2 relative to the adult individuals of their own species. Such a

232 distribution in the morphospace defined by PC1-2 suggests similar ontogenetic trajectories for

233 the two species.

234

235 ***Intraspecific variation of skull shape in nine-banded armadillos***

236 In specimens for which sex was available (22 females and 32 males for the mandible; 19 females

237 and 34 males for the cranium), a MANOVA shows that there is no sexual dimorphism present in

238 the cranial data (Wilks' lambda=0.2429, F=1.514, p=0.182), so sex is unlikely to be responsible

239 for the variation observed in the cranium of *D. novemcinctus*, although it might partly account

240 for the variation in the mandible (Wilks' lambda=0.2292, F=2.579, p=0.011). ANOVAs also

241 show that there is no relationship between sex and size (mandibles, F=0.4219, p=0.52; crania,

242 F=0.00143, p=0.97). A multivariate regression of the shape component on size was significant

243 (mandible, Wilks' lambda=0.3468, F=3.454, p <0.001; cranium, Wilks' lambda=0.1447,

244 F=8.446, p <0.001). When looking at the allometric shape vectors obtained with the centroid size

245 (Figure S1), we found that size explains 14.14% and 14.32% of the variation in the whole

246 mandibular and cranial data sets respectively. Shape data corrected for allometry are presented in

247 Figures S3 and S4.

248   A weak intraspecific differentiation (per country) is noticeable in the mandibular

249 morphology data (Wilks' lambda=0.0001404, F=1.523, p <0.001; Fig. 5A). The first principal

250 component (9.87% of total shape variation) weakly discriminates specimens from Brazil,

251 Bolivia, Paraguay, Uruguay (positive values) from other specimens (negative values). This axis

252 separates mandibles characterized by a robust and short horizontal ramus, a long ascending

253 ramus, a high coronoid process, a low condylar process, and a poorly individualized angular

254 process, from mandibles with a slender and elongated horizontal ramus, a short ascending ramus,

255 a low coronoid process, a high condylar process, and a well individualized angular process (Fig.

256 5A). In terms of shape variation, PC2 (4.745% of total shape variation) separates mandibles that

257 show an elongated anterior part of the horizontal ramus, a short tooth row, and a high and

258 distally oriented coronoid processes, from mandibles having a reduced anterior part of the

259 horizontal ramus, an elongated tooth row, and a low coronoid process. We observed even less

260 differentiation with shape data corrected for allometry (Figure S3), which indicates that some

261 specimens differ significantly in size. This is confirmed by a regression of the first principal

262 component on the logarithm of the centroid size (Fig. 5B), which shows that the specimens from

263 Brazil, Uruguay, Paraguay, Bolivia, Peru, Ecuador, Costa Rica, and Colombia are usually

264 smaller.

265   A MANOVA was also used to explore if the cranial variation matches the geographical

266 distributions of *D. novemcinctus* (Wilks' lambda=2.97x10^{-6}, F=2.157, p <0.001). When looking

267   at the cranial morphological variation according to geographic origin (*i.e.*, countries) (Fig. 6),

268   several trends can be observed. PC1, accounting for 22.7% of the overall variation, demonstrates

269   a change in how domed the dorsal surface of the skull is, and positively correlates with an

270   increase in snout length, a decrease in braincase size, jugals that are more extended

271   dorsoventrally, and shorter pterygoid processes (Fig. 6A). Specific clusters are recognizable on

272   the first principal component, with specimens from Brazil, Paraguay, Venezuela (NMNH 406700

273   from Clarines area, North), Ecuador (BMNH-14-4-25-86 from Gualaquiza, South East),

274   Colombia (AMNH 136252 from Villavicencio area, Centre), Peru, Bolivia, Paraguay, and

275   Uruguay that congregate in the negative values, whereas all other specimens lay in the positive

276   values. PC2 is responsible for 8.6% of the variance, and describes variation in the size of the

277   posterior part of the rostrum; it also displays variation in length of the posterior part of the palate

278   with an anterior border of the palatine that is well behind the posterior end of the tooth row in

279   skulls showing positive values. This axis mainly separates specimens from USA, Mexico, Belize,

280   Honduras, Guatemala, and Nicaragua (negative values) from other specimens (positive values).

281   We observed less specific differentiation with shape data corrected for allometry (Figure S4),

282   which shows that the different geographical subgroups differ significantly in size. This is

283   confirmed by a regression of the first principal component to the logarithm of the centroid size

284   (Fig. 7).

285   A Linear Discriminant Analysis (LDA) of shape coordinates was performed in order to

286   take into account the entirety of morphological variation (*i.e.*, 35 first PCs that represent 90.6%

287   of the variance) and to maximize discrimination among specimens belonging to different

288   countries. Only countries for which we had several specimens could be considered here. Three

289   main regional groups were clearly recovered by the analysis (Fig. 8A): a Northern morphotype, a

290 Southern morphotype, and a group restricted to the Guiana Shield (GS). The first group from

291 North and Central America includes specimens from the US, Mexico, Guatemala, and Belize.

292 The South American group gathers specimens from Brazil, Uruguay, Bolivia, Peru, Colombia,

293 and Venezuela. Finally, specimens from French Guiana, Suriname, and Guyana congregate in a

294 last distinctive group. Some specimens from Colombia, Venezuela, and Ecuador do not gather

295 with any of those groups and sit in the middle of the graph defined by the first two discriminant

296 axes; these specimens are, however, well discriminated on the third and fourth discriminant axes

297 (Fig. 8B) and might constitute a fourth individualized regional group among *D. novemcinctus*,

298 called hereafter the Central morphotype.

299   The discriminant model used to separate the regional groups, based on artificial

300 boundaries (i.e. borders of countries), was checked using a classification phase. The same

301 procedure was then used on under-sampled countries (*i.e.*, when n=1) to assess their affiliation to

302 one of the four abovementioned groups. This analysis showed 95% correct classification of

303 specimens (Table S2). Most regional misclassifications were with specimens coming from the

304 limit of the distribution range of the groups. Two Brazilian specimens from Amapa are put

305 together with the Guianan specimens (Table S2) and confirm previous results from the PCA,

306 where these two specimens clearly depart from the rest of the Brazilian specimens (Fig. 6A).

307 Three specimens from Venezuela (NMNH 406700 from Clarines area, North), Ecuador (BMNH-

308 14-4-25-86 from Gualaquiza, South East), and Colombia (AMNH 136252 from Villavicencio

309 area, Centre) were *a posteriori* classified as close to the Southern morphotype. All these

310 specimens were collected East of the Andes (Fig. 9) and grouped with Brazilian specimens in the

311 PCA analyses. Concerning the countries for which only one specimen was available, the

312 classification analyses gave congruent results with the grouping proposed by the principal

313   component analysis: specimens from Paraguay and Peru were classified as being part of the

314   Southern morphotype, whereas specimens from Nicaragua, Honduras, and Costa Rica were

315   classified as grouping with the Northern morphotype (Table S2). Using a reduced set of

316   landmarks, the specimen from Panama was attributed to the Central morphotype. When

317   performing these classification methods using the four groups as factors (*i.e.*, Northern, Central,

318   Southern, and Guianan morphotypes; see Table S3), instead of countries, we retrieved 100%

319   correct classification of specimens.

320   We performed similar analyses (PCA and LDA, see Figure S5) using linear cranial

321   measurements traditionally used in systematic studies. In all cases, these analyses failed to

322   retrieve a clear-cut discrimination between the four groups defined above.

323

Discussion

Morphological variation of skull among Dasypus *species*

326   Skull ratios are commonly used to compare *Dasypus* species, especially the length of the palate

327   to the length of the skull (PL/CNL), and the length of the rostrum to the length of the skull (RL

328   adj./CNL) (Wetzel, 1985). Three subgenera are commonly recognized on this basis:

329   *Cryptophractus* (including *D. pilosus*), *Hyperoambon* (including *D. kappleri*), and *Dasypus*

330   (including all remaining species) (Wetzel & Mondolfi, 1979). Our results are largely consistent

331   with findings from previous studies regarding existing differences among *Dasypus* species.

332   Allometry substantially explains cranial differences, with the exception of *D. pilosus*, which does

333   not follow the main dasypodine allometric trend (Figs. 3 and 4). The hairy long-nosed armadillo

334   is clearly distinguished from the other four *Dasypus* species studied by a lengthening of the snout

335   and mandible and a lesser development of the braincase and basicranium. All these

336   characteristics might be linked to their unique diet, which predominantly includes ants and

337   termites (Castro et al., 2015). Considering these distinctive morphological features and the

338   specific structure of its osteoderms, Castro et al. (2015) recently proposed including *D. pilosus* in

339   a different genus, *Cryptophractus*. However, recent molecular results (Gibb et al., 2016) did not

340   support such a taxonomic reassessment and argued for the retention of the hairy long-nosed

341   armadillo in the genus *Dasypus*. *D. pilosus* thus likely represents a case of rapid acquisition (*i.e.*,

342   2.8 Ma as estimated by Gibb et al., 2016) of distinctive morphological traits in line with the shift

343   to a divergent behaviour, ecology, and high altitude habitat.

344   Both molecular and morphological data suggested that *D. kappleri* is broadly separated

345   from the other *Dasypus* species (Wetzel & Mondolfi, 1979; Gibb et al., 2016), but contrary to

346   results of Castro et al. (2015) in which it is the crown group. Mitogenomic data clearly identified

347   *D. kappleri* as the sister group to all other *Dasypus* species, from which it diverged more than 12

348   million years ago (Gibb et al., 2016), and Gibb et al. (2016) suggested placing it in the distinct

349   genus *Hyperoambon*, as originally proposed by Wetzel and Mondolfi (1979). *D. kappleri*

350   exhibited significant morphological differentiation in our results, with all the specimens

351   congregating in the morphospace at least in part because they are much larger than the other

352   species. However, the cranial morphology of *D. kappleri* still remains very close to that of *D.*

353   *novemcinctus* when compared to that of *D. septemcinctus*, *D. hybridus*, and *D. pilosus* (Fig. 4).

354   *D. kappleri* also grouped with *D. novemcinctus* to the exclusion of these latter taxa in Castro et

355   al. (2015). Recently, Feijo and Cordeiro-Estrela (2016) proposed recognizing three species

356   within *D. kappleri* based on morphological differences of the skull and carapace: *D. kappleri*

357   distributed in the Guiana shield; *D. pastasae* occurring from the eastern Andes of Peru, Ecuador,

358   Colombia, and Venezuela south of the Orinoco River into the western Brazilian Amazon; and

359   finally *D. beniensis* that occurs in the lowlands of the Amazonian Brazil and Bolivia to the south

360   of the Madre de Dios, Madeira, and the lower Amazon rivers. We only had access to a limited

361   number of specimens, but did not retrieve such a clear geographical segregation in shape (Figure

362   S6A), while we observed a mild differentiation in size with the Guianan *D. kappleri* usually

363   being bigger (Figure S6B).

364   Wetzel and Mondolfi (1979:47) placed *D. septemcinctus*, *D. hybridus*, and *D. sabanicola*

365   in the same subgenus together with *D. novemcinctus*. We observed that *D. hybridus* and *D.*

366   *septemcinctus* group together in the morphospace, but are largely separated from *D.*

367   *novemcinctus*. These two species are usually distinguished by external features, *D. hybridus*

368   possessing shorter ears and a longer tail than *D. septemcinctus* (Hamlett, 1939; Wetzel &

369   Mondolfi, 1979). Our morphometrical results showed that *D. hybridus* and *D. septemcinctus*

370   display very similar cranial and mandibular morphologies. They also display several cranial

371   characteristics in common with juvenile specimens of *D. novemcinctus*. Such morphological

372   similarities echo recent molecular findings (Gibb et al., 2016) which showed that mitogenomic

373   sequences of *D. hybridus* were almost identical to those of an Argentinian *D. septemcinctus*

374   (99.3% identity). The two species were considered as valid based on cranial and body

375   measurements (Hamlett, 1939; Wetzel, 1985) despite the fact that they display many external

376   resemblances and have overlapping geographical distributions. A recent study of their internal

377   cranial sinuses also failed to provide diagnostic characters for distinguishing these two species

378   (Billet et al., unpublished data). Our samples were very limited for both *D. hybridus* (n=4) and

379   *D. septemcinctus* (n=3), but additional sampling will undoubtedly help to define the systematic

380   status of the two species.

381   We did not have access to the two most recently recognized *Dasypus* species: the

382   Yunga's lesser long-nosed armadillo *D. mazzai* (Yepes, 1933; Vizcaíno, 1995; Feijo & Cordeiro-

383   Estrela, 2014), and the northern long-nosed armadillo *D. sabanicola* (Mondolfi, 1967). The

384   validity of the former was and is still hotly debated (Wetzel & Mondolfi, 1979; Vizcaíno, 1995;

385   Gardner, 2008; Feijo & Cordeiro-Estrela, 2014), while the specific status of the latter also

386   remains controversial (Wetzel & Mondolfi, 1979; Wetzel, 1985). Cranial morphometric data

387   might provide useful insights into the systematic status of the two species.

388

389   ***Morphological systematics and skull shape variation in* Dasypus novemcinctus**

390   Relative skull shape has previously been examined for systematic purposes in the genus

391   *Dasypus*, but never with a focus on patterns of intraspecific variation. Hamlett (1939) cast doubt

392   on the possibility of reliably identifying different subgroups within *D. novemcinctus*, although

393   early workers had already recognized several, either at a specific or at a subspecific level. Peters

394   (1864) described *Dasypus fenestratus* from Costa Rica based on the position of the small and

395   numerous major palatine foramina, some of which are connected to the incisive foramina

396   through a groove between (not in front of) the anterior teeth, as well as its medially shorter

397   maxillo-palatine bones, the position of the palatine suture posterior to the end of the tooth row,

398   the position of the lacrimal foramen closer to the orbital rim, and one character related to the

399   extent of the pelvic shield of the carapace. Gray (1873) tentatively recognized as many as seven

400   species of nine-banded armadillos in South and Central Americas, among which five were new:

401   *Tatusia* (=*Dasypus*) *granadiana*, *T. leptorhynchus*, *T. brevirostris*, *T. leptocephala*, and *T.*

402   *boliviensis*. He also followed Peters (1864) and recognized *T. mexicana* (a variety of *D.*

403   *novemcinctus* in Peters 1864), but decided to ignore *T. fenestratus*. Both Peters (1864) and Gray

404   (1873) used a very small number of specimens, and Gray (1873) distinguished all these species

405   based mainly on the morphology of the lacrimal bones and minute morphological variations of

406   the head scutes. Allen (1911) later considered *D. fenestratus* and *D. mexicanus* as synonyms at

407   the subspecific level (*D. novemcinctus fenestratus* Peters). He also described *D. novemcinctus*

408   *hoplites* from Grenada, a subspecies that he considered to be distinctly characterized by a shorter

409   tooth row, due to the absence of the last tooth locus.

410   From the inspection of a series of specimens from Panama, Costa Rica, and Yucatan,

411   Allen (1911) also distinguished a Central American morphotype. Compared to Brazilian

412   specimens, Allen's Central American armadillo was characterized by short palatine bones that

413   did not reach the level of the most posterior teeth, an obvious inflation of the maxillary region

414   located in front of the lacrimal bone, and a lateral margin of the skull that was largely convex at

415   the level of the second or third tooth in ventral view. Based on size differences, Hagmann (1908)

416   described the subspecies *D. n. mexianae*, which he thought was restricted to a small area close to

417   the mouth of the Amazon River. Lönnberg (1913) defined *D. n. aequatorialis* from Ecuador,

418   which McBee and Baker (1982) later proposed considering a probable synonym to *T.*

419   *granadiana* Gray 1873. Lönnberg's comparisons were based on morphological characteristics of

420   the carapace, *D. n. aequatorialis* showing differences in the occipital portion of the frontal

421   shield, as well as different proportions of the scales of the shoulder and pelvic shields. Later on,

422   Russell (1953) proposed recognizing two subspecies in Mexico: *D. n. davisi* in the northwestern

423   part of Mexico, and *D. n. mexicanus* in the remaining part of the country. Even if it is close

424   morphologically to *D. n. mexicanus*, *D. n. davisi* is much smaller in size, and displays a few

425   distinctive features, such as small maxillary teeth, a narrow mandible with a posteriorly projected

426   angular process, and differences in suture closure patterns and shape, for instance with a parietal-

427   frontal sutures that lies well behind the posterior process of the zygomatic arch (Russell, 1953).

428   Most of these early descriptions, be they at a specific or subspecific level, were based on subtle

429   morphological differences. No proper quantification of the skull variation was undertaken up

430   until now.

431   Our statistical analysis of skull shape demonstrated that *D. novemcinctus* exhibits a

432   significant level of intraspecific variation, with several clearly identified subgroups. Our

433   multivariate analyses suggest the absence of sexual dimorphism in the shape of the cranium and

434   a slight sexual dimorphism in the mandibular morphology. McBee & Baker (1982) proposed that

435   male nine-banded armadillos tend to be slightly larger than females. However, Loughry &

436   McDonough (2013) pointed out that McBee and Baker based this assertion on a paper that only

437   examined a very small number of animals, and reach the more general conclusion that there is no

438   sexual dimorphism in this species using measurements of hundreds of animals. Our univariate

439   analyses confirmed the absence of size differences between females and males *D. novemcinctus*.

440   We show that allometry is likely to explain a substantial part of the observed morphological

441   variation, including the geographical variation. Our morphometric analysis revealed distinct

442   geographical differentiation among nine-banded armadillos, both in size and shape. This echoes

443   early findings by Wetzel and Mondolfi (1979) who already pointed out size gradients among

444   different populations of *D. novemcinctus*. Interestingly, our geometric morphometric analyses

445   permitted us to define four discrete phenotypic units. These units display very different cranial

446   characters and occupy very distinct geographical distributions, which are in essence allopatric.

447   Specimens from Brazil, Uruguay, Paraguay, Bolivia, Peru, and from regions of Ecuador,

448   Colombia, and Venezuela located east of the Andes make up most of one group and show a very

449   stable pattern of variation (Fig. 9). They are on average smaller than the three remaining groups.

450   Loughry & McDonough (1998) already showed that body size of armadillos from Poco das

451   Antas (Brazil) was smaller than that of animals from the United States. Skulls of this Southern

452   morphotype are characterized by smaller and flatter skulls with short frontal sinuses, a narrow

453   snout with short premaxillary bones, a narrow interorbital width, a long and slender jugal part of

454   the zygomatic arch, long pterygoid processes, and a basicranium aligned with the palate in lateral

455   view (Fig. 6). We found no sign of morphological differentiation of specimens from the mouth

456   of the Amazon River, despite of the recognition of the subspecies *D. n. mexianae* (Hagmann,

457   1908). The area covered by the specimens attributed to this morphological unit fully

458   encompasses the Amazon basin and seemed to be delimitated by the Andes on the western side.

459   As a matter of fact, the single Ecuadorian specimen coming from the eastern side of the Andes

460   appeared to be distinct from most other Ecuadorian specimens, but morphologically close to

461   Brazilian and Bolivian specimens. The same holds true for the Peruvian, Colombian, and

462   Venezuelan specimens collected east of the Andes. The distribution of this group is reminiscent

463   of that of the subspecies *D. novemcinctus novemcinctus* Linnaeus, except for the Guiana Shield

464   area (Gardner, 2008). It also recalls a similar lineage molecularly identified (Arteaga et al.,

465   unpublished data) and the Southern morphotype evidenced by the analysis of paranasal spaces

466   (Billet et al., unpublished data). Unfortunately the type specimen of *D. novemcinctus*, which is

467   supposedly housed in the Swedish Museum of Natural History in Stockholm (Lönnberg, 1913),

468   could not be included in our analyses. The type locality of *Dasypus novemcinctus* Linnaeus is

469   "America meridionali" and is generally thought to be from the eastern coast of Brazil (Allen,

470   1911).

471   The next differentiated group is represented by individuals originating from the Guiana

472   shield region, including French Guiana, Guyana, Suriname, and Amapa in Brazil (Fig. 9). All the

473   specimens belonging to this Guianan morphotype display large dome-shaped skulls that share

474   distinctive morphological features, including long frontal sinuses, a wide snout with long

475   premaxillary bones, a large interorbital width, large lacrimal bones, a short and massive jugal

476   part of the zygomatic arch, an anterior border of the palatine located well behind the posterior

477   end of the tooth row, short pterygoid processes, and a basicranium situated above the palatal

478   plane (Fig. 6). Studies of paranasal sinuses affirm the distinctness of this group and show that the

479   dome-shaped frontal region of Guianan nine-banded armadillos is occupied by a

480   characteristically inflated pair of frontal sinuses that extend posteriorly to the fronto-parietal

481   suture (Billet al., unpublished data). No subspecies has ever been recognized or proposed in this

482   part of South America, and such a clear-cut morphological divergence of Guianan specimens of

483   *D. novemcinctus* is here proposed for the first time. These morphometric findings corroborate

484   recent molecular studies, which showed that specimens from French Guiana are very distant

485   from the US populations (Huchon et al., 1999) and represent a distinct branch in the dasypodine

486   mitogenomic tree (Gibb et al., 2016).

487   The distribution of the third recognized morphological group is more limited. It is

488   distributed from the western Andes of Ecuador and Colombia to Venezuela, and Panama (Fig.

489   9). This Central morphotype is characterized by high and short skulls having moderately

490   developed frontal sinuses, long premaxillary bones, a narrow interorbital width (wider than

491   Southern specimens but narrower than Guianan specimens), a massive anterior part of the

492   zygomatic arch that is much larger than the posterior part, a short and high jugal part of the

493   zygomatic arch that is largely convex ventrally, an anterior border of the palatine located well

494   behind the posterior end of the tooth row, short pterygoid processes, and a basicranium well

495   above the palatal plane (Fig. 6). This distribution roughly corresponds to the combined ranges of

496   two previously described subspecies, *D. n. fenestratus* (Peters, 1864) and *D. n. aequatorialis*

497   (Lönnberg, 1913) suggesting that these subspecies might be synonymous. However, we could

498   not fully test this hypothesis since we had access to only one specimen from west of the Andes in

499   Peru, Ecuador and southern Bolivia. Studies on the paranasal spaces (Billet et al., unpublished

500   data) failed to recognize such a group, and instead grouped some specimens from these regions

501   with specimens from North and Central America, whereas others (from the western parts of

502   Colombia, Venezuela and from Panama) could not confidently be referred to a given frontal

503   sinus morphotype. In contrast, molecular studies recovered a lineage similar to the group

504   recognized here, distributed from the Northern Andes to Central America and then expanding

505   into western Mexico (Arteaga et al., 2012).

506   The last distinct morphotype occurs from Nicaragua to the southeastern part of the US

507   (Fig. 9). The range of this Northern morphotype spans the proposed distribution areas of the

508   subspecies *D. n. mexicanus* and *D. n davisi*, as well as the northernmost part of the distribution

509   range of *D. n. fenestratus*. All the skulls from this area display moderately developed frontal

510   sinuses convergent toward the midline, long premaxillary bones, a narrow interorbital width

511   (wider than Southern specimens but narrower than Guianan specimens), a long and slender jugal

512   part of the zygomatic arch that is largely convex ventrally, an anterior border of the palatine

513   located at the level of the posterior end of the tooth row, short pterygoid processes, and a

514   basicranium slightly above the palatal plane (Fig. 6). Contrary to Russell (1953), we did not find

515   major morphological cranial differences between north-western and eastern Mexican

516   populations. Our results thus cast doubts on the validity of the subspecies *D. n. davisi*. The

517   morphological homogeneity in this group is also at odds with the presence of two mitochondrial

518   lineages in Mexico (Arteaga et al., 2012), but is consistent with the presence of nuclear gene

519   flow between them (Arteaga et al., 2011). This Northern group includes the invasive US

520   armadillo population, which is derived from two geographical sources: one from Mexico, and

521   one from south-central Florida, where captive animals were presumably released (Loughry &

522   McDonough, 2013). Echoing the results obtained on six microsatellite loci described by Loughry

523   et al. (2009), our findings indicate a close relationship between the two US populations. The

524   recognition of this Northern unit with individuals ranging from Central to the southeastern US is

525   also in agreement with their distinctive pattern of paranasal sinuses (Billet et al., unpublished

526   data).

527   The newly recognized subgroups within *D. novemcinctus* prompt questions about the role

528   of ecological factors likely to have influenced their morphological differentiation. Variation in

529   skull morphology as a result of ecological factors has been studied in a number of species over

530   recent years (*e.g.*, Caumul and Polly, 2005; Wroe and Milne, 2007; Hautier et al., 2012). Factors

531   such as temperature, diet and competition may cause phenotypic variation and are likely to

532   explain some morphological differences among the identified groups. These ecological factors

533   vary in relation to geography, and differences in geographical distribution can drive selection for

534   different phenotypes, which may eventually lead to distinctive populations or even new species.

535   Since the four *D. novemcinctus* subgroups are not sympatric in most of their respective natural

536   ranges, we can hypothesize that environment and/or genetic drift, but not competition, may be

537   responsible for some of the observed intraspecific variation. The northern Andes constitute a

538   clear geographical barrier, which limited contacts between northern/central and southern

539   populations, and thus has likely played a major role in shaping the morphological differentiation

540   of the long-nosed armadillos. This biogeographical barrier seems to have played a significant

541   role in xenarthran evolution and diversification in general (Moraes-Barros & Arteaga, 2015),

542 since it also marks the separation between the two living species of tamanduas, with *Tamandua*

543 *mexicana* in the north and *T. tetradactyla* in the south (Superina, Miranda & Abba, 2010), as

544 well as between two living species of within naked-tailed armadillos, with *Cabassous centralis*

545 in the north and *C. unicinctus* in the south (Abba & Superina, 2010).

546   The geographical distribution of the divergent populations of *D. novemcinctus* recalls the

547 pattern of morphological differentiation recently proposed for the greater long-nosed armadillo

548 (*D. kappleri*), especially for the Guianan specimens (Feijo & Cordeiro-Estrela, 2016). However,

549 in the nine-banded armadillo, we did not find a clear morphological differentiation within the

550 Amazonian basin, as defined by the opposite banks of the Madeira-Madre de Dios rivers (Feijo

551 & Cordeiro-Estrela, 2016), which separate *D. pastasae* from *D. beniensis*. Given the extent of

552 morphological variation reported within *D. kappleri*, Feijo and Cordeiro-Estrela (2016)

553 interpreted their findings as indicative of the fact that this species complex diverged earlier than

554 other *Dasypus* species, which would allow them to accumulate more differences. Such a

555 hypothesis seems difficult to support, in view of the substantial morphological variation

556 observed among different populations of *D. novemcinctus*, which have diverged more recently

557 (3.7 Ma, Gibb et al., 2016). Feijo and Cordeiro-Estrela (2016) also proposed that such

558 cumulative differences may result from strong environmental selective pressures. The newly

559 discovered morphological diversity within *D. kappleri* and *D. novemcinctus* is likely to represent

560 parallel cases of allopatric differentiation in response to diverging environmental pressures. In

561 both cases, only the future collecting of large-scale genomic nuclear data will allow testing of

562 these taxonomic proposals based on morphological data.

563

564 **Conclusions**

565   If our interspecific comparisons primarily just provide additional support for the current

566   designation of each group as a separate taxon, the intraspecific analyses of variation within *D.*

567   *novemcinctus* enable detection of previously overlooked morphotypes. Our study of the

568   intraspecific variation of the skull in *D. novemcinctus* reveals clear links to geographic

569   distribution, and allows a revision of past taxonomic delimitations. Based on the cranial

570   differences observed, we consider that *D. novemcinctus* should be regarded either as a polytypic

571   species (with three to four subspecies) or as a complex of several species (with three to four

572   species). A new unit of nine-banded armadillos from the Guiana Shield could be established,

573   which is in agreement with most recent investigations of molecular data and internal anatomy

574   (Loughry & McDonough, 2013; Billet G., unpublished data). At this stage, we refrain to make

575   definitive taxonomic pronouncements for the four morphological subsets in the absence of a

576   more exhaustive molecular sampling allowing a complete taxonomic reassessment of the genus

577   (Arteaga M-C., unpublished data). The discovery of divergent populations within *D.*

578   *novemcinctus* has implications for conservation of the species. In some areas, human activities

579   have led to habitat degradation and fragmentation (Zimbres et al., 2013) or even to habitat loss.

580   These divergent populations may be under threat and may require specific conservation

581   measures, or at least a close re-examination of their conservation status. If we were to consider

582   them as separate management units and not as a single species with a large distribution, the

583   threat of endangerment to *D. novemcinctus* may merit re-evaluation, since it is currently

584   classified globally as 'Least Concern' by the IUCN (Loughry, McDonough & Abba, 2014). In

585   addition, our results demonstrate that specimens of *D. novemcinctus* should be chosen with

586   caution when making anatomical comparisons or performing cladistic analyses (*e.g.*, Castro et

587   al., 2015); their geographical distribution should be at least specified in all cases. Lastly,

588 morphological investigation of intra- and interspecific variation in *Dasypus* needs to be extended

589 to the other parts of the body, the carapace in particular. The cranial differences detected among

590 the defined groups might be linked to previously detected differences in the number and shape of

591 scutes on the head shield (*e.g.*, Lönnberg, 1913), for example. Geometric morphometric data

592 holds out the possibility of effectively studying covariation patterns among osteological parts and

593 features of the carapace. Given the quality of the cingulate fossil record, using geometric

594 morphometric methods seems likely to be equally useful on extinct forms, and so might also

595 provide fruitful ways to interpret past morphological diversity.

596

597 **Acknowledgements**

598 We are grateful to Christiane Denys, Violaine Nicolas, and Géraldine Véron, (Muséum National

599 d'Histoire Naturelle, Paris, France), Roberto Portela Miguez, Louise Tomsett and Laura Balcells

600 (British Museum of Natural History, London, UK), Eileen Westwig (American Museum of

601 Natural History, New-York, USA), Burton Lim (Royal Ontario Museum, Toronto, Canada),

602 Nicole Edmison and Chris Helgen (National Museum of Natural History, Washington, DC,

603 USA), Jake Esselstyn (Louisiana State University, Museum of Natural Sciences, Bâton-Rouge,

604 USA), Manuel Ruedi (Muséum d'Histoire naturelle, Geneva, Switzerland), Claudia Regina da

605 Silva (Instituto de Pesquisas Científicas e Tecnológicas do Estado do Amapá, Macapá, Brazil),

606 Steven van der Mije (Naturalis Biodiversity Center, Leiden, Netherland), François Cazeflis and

607 Suzanne Jiquel (Institut des Sciences de l'Evolution, Montpellier, France), Lucile Dudoignon

608 (KWATA association, Cayenne, France), Dominique Charles (CNRS, Montpellier, France),

609 Maria-Clara Arteaga, Maria Nazareth da Silva (Instituto de Pesquisas Científicas e Tecnológicas

610 do Estado do Amapá, Macapá, Brazil) for access to comparative material. We thank Clara

611 Belfiore for her help in the data acquisition and Rémi Lefebvre for interesting discussions on the

612 dataset. R. Lebrun (Institut des Sciences de l'Evolution, Montpellier, France), Farah Ahmed

613 (British Museum of Natural History, London, UK), Miguel García-Sanz and Florent Goussard

614 (Platform AST-RX MNHN, Paris, France) generously provided help and advice on the

615 acquisition of CT scans. Some of the experiments were performed using the µ-CT facilities of

616 the Montpellier Rio Imaging (MRI) platform and of the LabEx CeMEB. In compliance with

617 Advantages and Benefits Sharing policy in French Guiana, material from French Guiana has

618 been registred in the collection JAGUARS (http://kwata.net/la-collection-jaguars-pour-l-etude-

619 de-la-biodiversite.html; CITES reference: FR973A) supported by Kwata NGO, Institut Pasteur

620 de la Guyane, DEAL Guyane, and Collectivité Territoriale de la Guyane. This is contribution

621 ISEM 2017-XXX of the Institut des Sciences de l'Evolution.

622

References

624 Abba AM., Superina M. 2010. The 2009/2010 armadillo Red List assessment. *Edentata* 11:135–

625   184.

626 Allen G. 1911. Mammals of the West Indies. *Bulletin of the Museum of Comparative Zoology*

627   54:175–263.

628 Arteaga MC., McCormack JE., Eguiarte LE., Medellín RA. 2011. Genetic admixture in

629   multidimensional environmental space: asymmetrical niche similarity promotes gene flow

630   in armadillos (*Dasypus novemcinctus*). *Evolution* 65:2470–2480.

631 Arteaga MC., Piñero D., Eguiarte LE., Gasca J., Medellín R. 2012. Genetic structure and

632   diversity of the nine-banded armadillo in Mexico. *Journal of Mammalogy* 93:547–559.

633 Asher RJ., Lehmann T. 2008. Dental eruption in afrotherian mammals. *BMC biology* 6:14. DOI:

634   10.1186/1741-7007-6-14.

635   Bookstein F. 1991. *Morphometric Tools for Landmark Data. Geometry and biology*. Cambridge:

636   Cambridge University Press.

637   Carlini AA., Castro MC., Madden RH., Scillato-Yané GJ. 2013. A new species of Dasypodidae

638   (Xenarthra: Cingulata) from the late Miocene of northwestern South America: implications

639   in the Dasypodini phylogeny and diversity. *Historical Biology*:37–41. DOI:

640   10.1080/08912963.2013.840832.

641   Carlini AA., Vizcaíno SF., Scillato-yané GJ. 1997. Armored xenarthrans: a unique taxonomic

642   and ecologic assemblage. In: Kay R, Madden R, Cifelli R, Flynn J. eds. *Vertebrate*

643   *Paleontology in the Neotropics. The Miocene Fauna of La Venta, Colombia*.

644   Washington/London: Smithsonian Institution Press, 213–226.

645   Castro MC. 2015. Sistemática y evolución de los armadillos Dasypodini (Xenarthra, Cingulata,

646   Dasypodidae). *Revista del Museo de La Plata* 15:1–50.

647   Castro MC., Avila LS., Freitas ML., Carlini AA. 2013a. The armadillo *Propraopus sulcatus*

648   (Mammalia: Xenarthra) from the late Quaternary of northern Brazil and a revised synonymy

649   with *Propraopus grandis*. *Quaternary International* 317:80–87. DOI:

650   10.1016/j.quaint.2013.04.032.

651   Castro MC., Carlini AA., Sánchez R., Sánchez-Villagra MR. 2014. A new Dasypodini armadillo

652   (Xenarthra: Cingulata) from San Gregorio Formation, Pliocene of Venezuela: affinities and

653   biogeographic interpretations. *Naturwissenschaften* 101:77–86. DOI: 10.1007/s00114-013-

654   1131-5.

655   Castro MC., Ciancio MR., Pacheco V., Salas-Gismondi RM., Bostelmann JE., Carlini AA. 2015.

656   Reassessment of the hairy long-nosed armadillo *"Dasypus"pilosus* (Xenarthra,

657   Dasypodidae) and revalidation of the genus *Cryptophractus* Fitzinger, 1856. *Zootaxa*

658   3947:30–48. DOI: 10.11646/zootaxa.3947.1.2.

659   Castro MC., Ribeiro AM., Ferigolo J., Langer MC. 2013b. Redescription of *Dasypus punctatus*

660   Lund, 1840 and considerations on the genus *Propraopus* Ameghino, 1881. *Journal of*

661   *Vertebrate Paleontology* 33:434–447. DOI: 10.1080/02724634.2013.729961.

662   Caumul R., Polly P. 2005. Phylogenetic and environmental components of morphological

663   variation: skull, mandible, and molar shape in marmots (*Marmota*, Rodentia). *Evolution*

664   59:2460–2472.

665   Ciancio MR., Castro MC., Galliari FC., Carlini AA., Asher RJ. 2012. Evolutionary implications

666   of dental eruption in Dasypus (Xenarthra). *Journal of Mammalian Evolution* 19:1–8. DOI:

667   10.1007/s10914-011-9177-7.

668   Delsuc F., Superina M., Tilak M., Douzery EJP., Hassanin A. 2012. Molecular phylogenetics

669   unveils the ancient evolutionary origins of the enigmatic fairy armadillos. *Molecular*

670   *Phylogenetics and Evolution* 62:673–680. DOI: 10.1016/j.ympev.2011.11.008.

671   Dryden I., Mardia K. 1998. *Statistical Shape Analysis*. Chichester: John Wiley & Sons.

672   Feijo A., Cordeiro-Estrela P. 2014. The correct name of the endemic *Dasypus* (Cingulata:

673   Dasypodidae) from northwestern Argentina. *Zootaxa* 3887:88–94. DOI:

674   10.11646/zootaxa.3887.1.6.

675   Feijo A., Cordeiro-Estrela P. 2016. Taxonomic revision of the *Dasypus kappleri* complex, with

676   revalidations of *Dasypus pastasae* (Thomas, 1901) and *Dasypus beniensis* Lönnberg, 1942

677   (Cingulata, Dasypodidae). *Zootaxa* 4170:271–297. DOI: 10.11646/zootaxa.4170.2.3.

678   Gardner AF. 2008. *Mammals of South America, Volume 1, Marsupials, Xenarthrans, Shrews,*

679   *and Bats*. Chicago and London: The University of Chicago Press.

680   Gaudin TJ., Wible JR. 2006. The phylogeny of living and extinct armadillos (Mammalia,

681   Xenarthra, Cingulata): a craniodental analysis. In: Carrano M, Gaudin TJ, Blob R, Wible JR

682   eds. *Amniote Paleobiology: Perspectives on the Evolution of Mammals, Birds and Reptiles*.

683   Chicago: The University of Chicago Press, 153–198.

684   Gibb GC., Condamine FL., Kuch M., Enk J., Moraes-Barros N., Superina M., Poinar HN.,

685   Delsuc F. 2016. Shotgun mitogenomics provides a reference phylogenetic framework and

686   timescale for living xenarthrans. *Molecular Biology and Evolution* 33:621–642. DOI:

687   10.1093/molbev/msv250.

688   Gray J. 1873. *Handlist of the Edentate, Thick-skinned, and Ruminant Mammals of the British*

689   *Museum*. London: British Museum of Natural History.

690   Hagmann G. 1908. Die Landsäugetiere der insel Mexiana. Als Beispiel der Einwirkung der

691   isolation auf die umbildung der arten. *Arch. Rass.-Gesell.-Biol. München* 5:1–32.

692   Hamlett G. 1939. Identity of *Dasypus septemcinctus* Linnaeus with notes on some related

693   species. *Journal of Mammalogy* 20:328–336.

694   Hammer Ø., Harper D., Ryan P. 2001. PAST: paleontological statistics software package for

695   education and data analysis. *Palaeontologica Electronica* 4:9.

696   Hautier L., Billet G., Eastwood B., Lane J. 2014. Patterns of morphological variation of extant

697   sloth skulls and their implication for future conservation efforts. *Anatomical Record*

698   297:979–1008. DOI: 10.1002/ar.22916.

699   Hautier L., Lebrun R., Cox PG. 2012. Patterns of covariation in the masticatory apparatus of

700   hystricognathous rodents: implications for evolution and diversification. *Journal of*

701   *morphology* 273:1319–37. DOI: 10.1002/jmor.20061.

702   Hensel R. 1872. *Beiträge zur Kenntnis der Säugethiere Süd-Brasiliens*. Berlin: lis den

703   Abhandlungen der Königl. Akademie der Wissenschaften.

704 Huchon D., Delsuc F., Catzeflis F., Douzery EJP. 1999. Armadillos exhibit less genetic

705   polymorphism in North America than in South America: nuclear and mitochondrial data

706   confirm founder effect in *Dasypus novemcinctus* (Xenarthra). *Molecular Ecology* 8:1743–

707   1748.

708 Lebrun R. 2008. Evolution and development of the strepsirrhine primate skull. University

709   Montpellier II and University of Zürich.

710 Lebrun R. 2014. ISE-MeshTools, a 3D interactive fossil reconstruction freeware. In: *12th Annual*

711   *Meeting of EAVP*. Torino,.

712 Lebrun R., Ponce de León M., Tafforeau P., Zollikofer C. 2010. Deep evolutionary roots of

713   strepsirrhine primate labyrinthine morphology. *Journal of Anatomy* 216:368–380.

714 Linnaeus C. 1758. *Systema Naturae, Ed; 10. L.* Uppsala: Salvii.

715 Lönnberg E. 1913. Mammals from Ecuador and related forms. *Arkiv för Zoologi* 8:1–36.

716 Loughry WJ., McDonough CM. 1998. Comparisons between nine-banded armadillo (Dasypus

717   novemcinctus) populations in Brazil and the United States. *Revista de biología tropical*

718   46:1173–1183.

719 Loughry WJ., McDonough CM. 2013. *The Nine-banded Armadillo: a Natural History*. Norman:

720   University of Oklahoma Press.

721 Loughry J., McDonough C., Abba A. 2014. *Dasypus novemcinctus*. *The IUCN Red List of*

722   *Threatened Species* 2014:e.T6290A47440785.

723 Loughry WJ., Truman RW., McDonough CM., Tilak M-K., Garnier S., Delsuc F. 2009. Is

724   leprosy spreading among nine-banded armadillos in the southeastern United States? *Journal*

725   *of Wildlife Diseases* 45:144–152. DOI: 10.7589/0090-3558-45.1.144.

726   McBee K., Baker RJ. 1982. *Dasypus novemcinctus*. *Mammalian Species* 162:1–9.

727   Mondolfi E. 1967. Descripción de un nuevo armadillo del género *Dasypus* de Venezuela

728   (Mammalia-Edentata). *Memorias de la Sociedad de Ciencias Naturales La Salle* 78:149–

729   167.

730   Moraes-Barros N., Arteaga MC. 2015. Genetic diversity in Xenarthra and its relevance to

731   patterns of Neotropical biodiversity. *Journal of Mammalogy* 96:1–13. DOI:

732   10.1093/jmammal/gyv077.

733   Peters W. 1864. Über neue Arten de Saugethier-gattungen *Geomys*, *Haplodon* und *Dasypus*.

734   *Monatsbericht der Königlich- Preussischen Akademie der Wissenschaften zu Berlin*

735   1865:177–181.

736   Rohlf F. 1999. Shape statistics: Procrustes superimpositions and tangent spaces. *Journal of*

737   *Classification* 16:197–223.

738   Russell R. 1953. Description of a new armadillo (*Dasypus novemcinctus*) from mexico with

739   remarks on geographic variation of the species. *Proceedings of the Biological Society of*

740   *Washington* 66:21–26.

741   Smith LL., Doughty RW. 1984. *The Amazing Armadillo: Geography of a Folk Critter*. Austin:

742   University of Texas Press.

743   Specht M. 2007. Spherical surface parameterization and its application to geometric

744   morphometric analysis of the braincase. University of Zürich Irchel.

745   Specht M., Lebrun R., Zollikofer C. 2007. Visualizing shape transformation between

746   chimpanzee and human braincases. *The Visual Computer* 23:743–751.

747   Superina M., Miranda FR., Abba AM. 2010. The 2010 anteater Red List assessment. *Edentata*

748   11:96–114.

749 Taulman JF., Robbins LW. 2014. Range expansion and distributional limits of the nine-banded

750   armadillo in the United States: an update of Taulman & Robbins (1996). *Journal of*

751   *Biogeography* 41:1626–1630.

752 Vizcaíno SF. 1995. Identificación especifica de las "mulitas", género *Dasypus* L. (Mammalia;

753   Dasypodidae); del noroeste argentino. Descripción de una nueva especie. *Mastozoologia*

754   *Neotropical* 2:5–13.

755 Wetzel R. 1985. Taxonomy and distribution of armadillos. In: Montgomery GG ed. *The*

756   *Evolution and Ecology of Armadillos, Sloths, and Vermilinguas*. Washington DC:

757   Smithsonian Institution Press, 23–46.

758 Wetzel R., Mondolfi E. 1979. The subgenera and species of long-nosed armadillos, genus

759   *Dasypus*. In: Eisenberg J ed. *Vertebrate Ecology in the Northern Neotropic*. Washington

760   DC: Smithsonian Institution Press, 43–63.

761 Wilson D., Reeder D. 2005. *Mammal Species of the World: a Taxonomic and Geographic*

762   *Reference. 3rd ed.* Baltimore: Johns Hopkins University Press.

763 Wroe S., Milne N. 2007. Convergence and remarkably consistent constraint in the evolution of

764   carnivore skull shape. *Evolution* 61:1251–1260.

765 Yepes J. 1933. Una especie nueva de "mulita" (Dasypodinae) para el norte argentino. *Physis*

766   11:225–232.

767 Zimbres B., Furtado MM., Jácomo, Anah T. A. Silveira L., Sollmann R., Tôrres NM., Machado

768   RB., Marinho-Filho J. 2013. The impact of habitat fragmentation on the ecology of

769   xenarthrans (Mammalia) in the Brazilian Cerrado. *Lanscape Ecology* 28:259–269.

770

771 **Table legends**

772   **Table 1.** Definitions of the landmarks used on the mandible.

773

774   **Table 2.** Definitions of the landmarks used on the cranium. Landmarks indicated with a star

775   were not used in the intraspecific comparisons.

776   **Figure Legends**

777

778   **Figure 1.** Landmarks digitized on the mandible and the skull. Dorsal (A), lateral (B), and ventral

779   views of the cranium; medial (C) and lateral (D) views of the mandible.

780

781   **Figure 2.** Illustration of the skull linear measurements. In blue, traditional measurements used in

782   Wetzel (1985). *Abbreviations*: LTC, length between the anterior tip of the nasal and the

783   posteriormost point of the supraoccipital; LR, rostral length; IOB, interorbital breadth; ILFB,

784   inter lacrimal foramina breadth; BB, distance between the left and right intersections between the

785   frontal, parietal, and squamosal sutures; NB, nasal breadth at the level of the nasal/frontal suture;

786   NL, nasal length; LCB, length between the anterior tip of the premaxillar and the condyles; TL,

787   length of the tooth row; PB, palate breadth posterior to the last premolar; BZP, distance between

788   the infraorbital and the maxillary foramina; MB, inter-meatus breadth; OCB, breadth between

789   the lateral border of the occipital condyle.

790

791   **Figure 3.** (**A**) Principal component analysis (PC1 *vs* PC2) and associated patterns of

792   morphological transformation for the mandible of five *Dasypus* species. (**B**) Regression of the

793   first principal component on the logarithm of the centroid size (R^2=0.23; p<0.001). *Symbols*:

794   blue squares, *D. kappleri*; black crosses, *D. novemcinctus*; green triangles, *D. hybridus*; green

795   diamonds, *D. septemcinctus*; red circles, *D. pilosus*.

796

797   **Figure 4.** (**A**) Principal component analysis (PC1 *vs* PC2) and associated patterns of

798   morphological transformation for crania of five *Dasypus* species. (**B**) Regression of the first

799   principal component on the logarithm of the centroid size (R^2=0.50; p<0.001). *Symbols*: blue

800   squares, *D. kappleri*; black crosses, *D. novemcinctus*; green triangles, *D. hybridus*; green

801   diamonds, *D. septemcinctus*; red circles, *D. pilosus*.

802

803   **Figure 5.** (**A**) Principal component analysis (PC1 *vs* PC2) and associated patterns of

804   morphological transformation for mandibles of *Dasypus novemcinctus*. (**B**) Regression of the

805   first principal component on the logarithm of the centroid size (R^2=0,035; p=0.03). *Symbols*:

806   green diamonds, Bolivia; green triangle, Brazil (solid green triangles are for specimens from

807   Amapa); green circles, Paraguay; green crosses, Peru; green squares, Uruguay; green bars,

808   Venezuela; blue diamonds, Belize; blue "plus", Guatemala; blue bars, Honduras; blue squares,

809   Mexico; blue crosses, Nicaragua; blue triangles, USA; blue circles, Costa Rica; black triangles,

810   Colombia; black crosses, Ecuador; black stars, Panama; orange squares, French Guiana; orange

811   crosses, Guyana; orange circles, Suriname.

812

813   **Figure 6.** Principal component analysis (**A**, PC1 *vs* PC2; **B**, PC3 *vs* PC4) and associated patterns

814   of morphological transformation for crania of *Dasypus novemcinctus*. *Symbols*: green diamonds,

815   Bolivia; green triangle, Brazil (solid green triangles are for specimens from Amapa); green

816   circles, Paraguay; green crosses, Peru; green squares, Uruguay; green bars, Venezuela; blue

817   diamonds, Belize; blue "plus", Guatemala; blue bars, Honduras; blue squares, Mexico; blue

818   crosses, Nicaragua; blue triangles, USA; blue circles, Costa Rica; black triangles, Colombia;

819   black crosses, Ecuador; orange squares, French Guiana; orange crosses, Guyana; orange circles,

820   Suriname.

821

822   **Figure 7.** Regression of the first cranial principal component (*Dasypus novemcinctus*) on the

823   logarithm of the centroid size (R^2=0.15; p<0.001). *Symbols*: green diamonds, Bolivia; green

824   triangle, Brazil (solid green triangles are for specimens from Amapa); green circles, Paraguay;

825   green crosses, Peru; green squares, Uruguay; green bars, Venezuela; blue diamonds, Belize; blue

826   "plus", Guatemala; blue bars, Honduras; blue squares, Mexico; blue crosses, Nicaragua; blue

827   triangles, USA; blue circles, Costa Rica; black triangles, Colombia; black crosses, Ecuador;

828   orange squares, French Guiana; orange crosses, Guyana; orange circles, Suriname.

829

830   **Figure 8.** Linear Discriminant Analysis (LDA) performed on cranial shape coordinates of

831   *Dasypus novemcinctus*. *Symbols*: green diamonds, Bolivia; green triangle, Brazil (solid green

832   triangles are for specimens from Amapa); green circles, Paraguay; green crosses, Peru; green

833   squares, Uruguay; green bars, Venezuela; blue diamonds, Belize; blue "plus", Guatemala; blue

834   bars, Honduras; blue squares, Mexico; blue crosses, Nicaragua; blue triangles, USA; black

835   triangles, Colombia; black circles, Costa Rica; black crosses, Ecuador; orange squares, French

836   Guiana; orange crosses, Guyana; orange circles, Suriname.

837

838   **Figure 9**. Summary map showing the geographical distribution of nine-banded armadillo

839   specimens investigated in this study and their attribution to one of the four main morphotypes

840   defined in this study: black, Central group; blue, Northern group; green, Southern group; orange,

841   Guianan group. Specimens lacking precise geographical information (other than country of

842   origin) are indicated with a square.

Figure 1

Figure 1

Landmarks digitized on the mandible and the skull. Dorsal (A), lateral (B), and ventral views
of the cranium; medial (C) and lateral (D) views of the mandible.

Figure 2

Figure 2

Illustration of the skull linear measurements. In blue, traditional measurements used in Wetzel (1985) . *Abbreviations*: LTC, length between the anterior tip of the nasal and the posteriormost point of the supraoccipital; LR, rostral length; IOB, interorbital breadth; ILFB, inter lacrimal foramina breadth; BB, distance between the left and right intersections between the frontal, parietal, and squamosal sutures; NB, nasal breadth; NL, nasal length; LCB, length between the anterior tip of the premaxillar and the condyles; TL, length of the tooth row; PB, palate breadth; BZP, distance between the infraorbital and the maxillary foramina; MB, inter-meatus breadth; OCB, breadth between the lateral border of the occipital condyle.
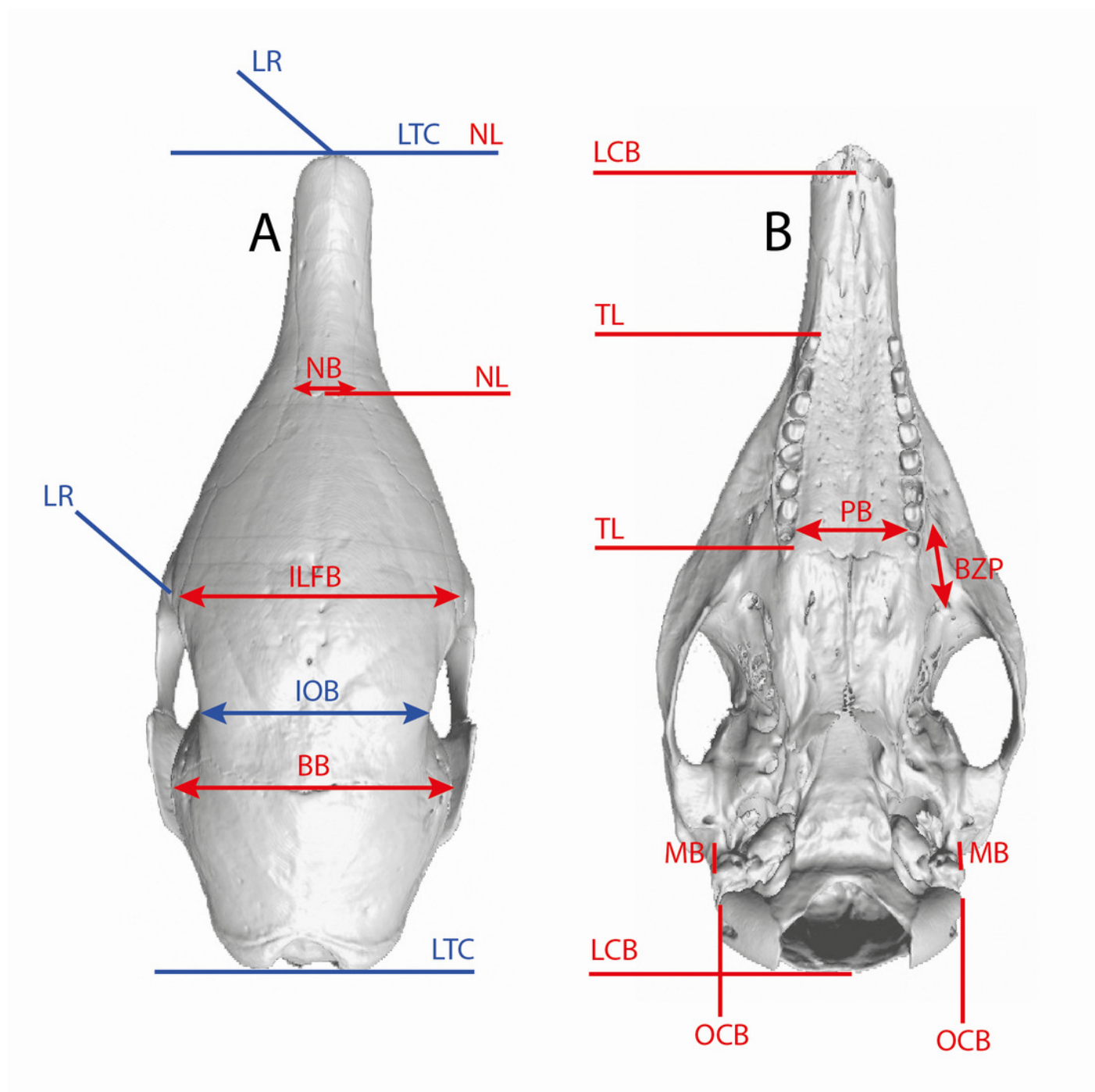
Figure 3

Figure 3

(**A**) Principal component analysis (PC1 *vs* PC2) and associated patterns of morphological transformation for the mandible of five *Dasypus* species. (**B**) Regression of the first principal component on the logarithm of the centroid size (R^2=0.23; $p<0.001$). *Symbols*: blue squares, *D. kappleri*; black crosses, *D. novemcinctus*; green triangles, *D. hybridus*; green diamonds, *D. septemcinctus*; red circles, *D. pilosus*.
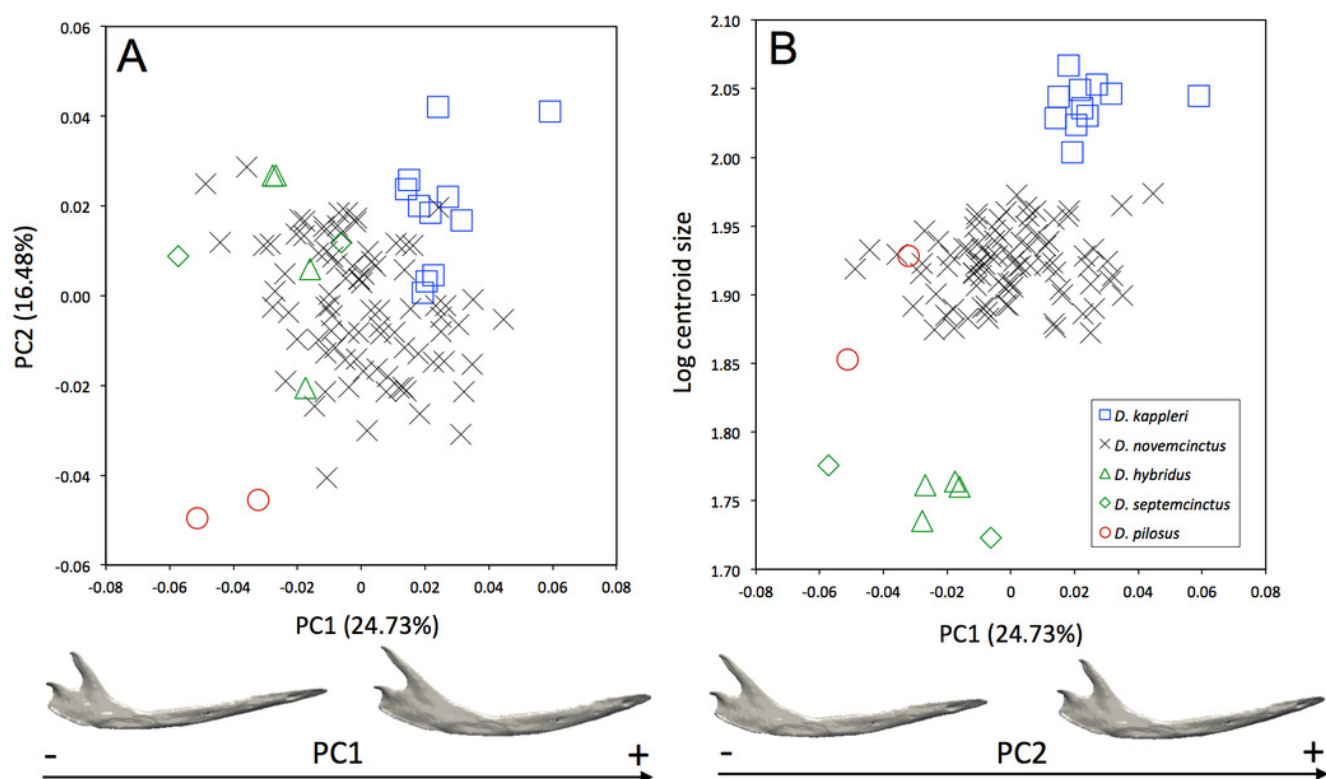
Figure 4

Figure 4

(**A**) Principal component analysis (PC1 *vs* PC2) and associated patterns of morphological transformation for crania of five *Dasypus* species. (**B**) Regression of the first principal component on the logarithm of the centroid size (R^2=0.50; p<0.001). *Symbols*: blue squares, *D. kappleri*; black crosses, *D. novemcinctus*; green triangles, *D. hybridus*; green diamonds, *D. septemcinctus*; red circles, *D. pilosus*.
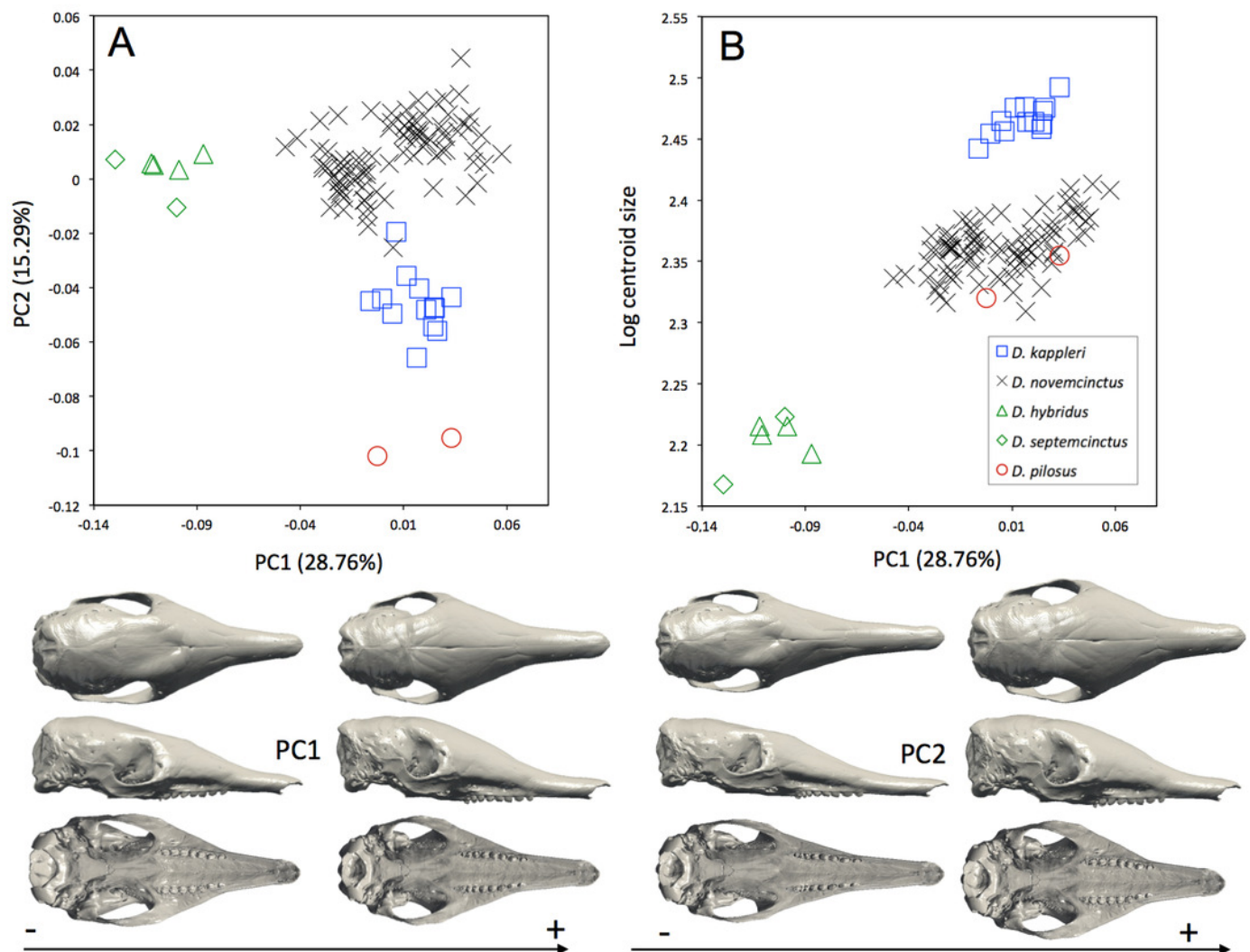
Figure 5

Figure 5

(**A**) Principal component analysis (PC1 *vs* PC2) and associated patterns of morphological transformation for mandibles of *Dasypus novemcinctus*. (**B**) Regression of the first principal component on the logarithm of the centroid size (R^2=0,035; p=0.03). *Symbols*: green diamonds, Bolivia; green triangle, Brazil (solid green triangles are for specimens from Amapa); green circles, Paraguay; green crosses, Peru; green squares, Uruguay; green bars, Venezuela; blue diamonds, Belize; blue "plus", Guatemala; blue bars, Honduras; blue squares, Mexico; blue crosses, Nicaragua; blue triangles, USA; blue circles, Costa Rica; black triangles, Colombia; black crosses, Ecuador; black stars, Panama; orange squares, French Guiana; orange crosses, Guyana; orange circles, Suriname.
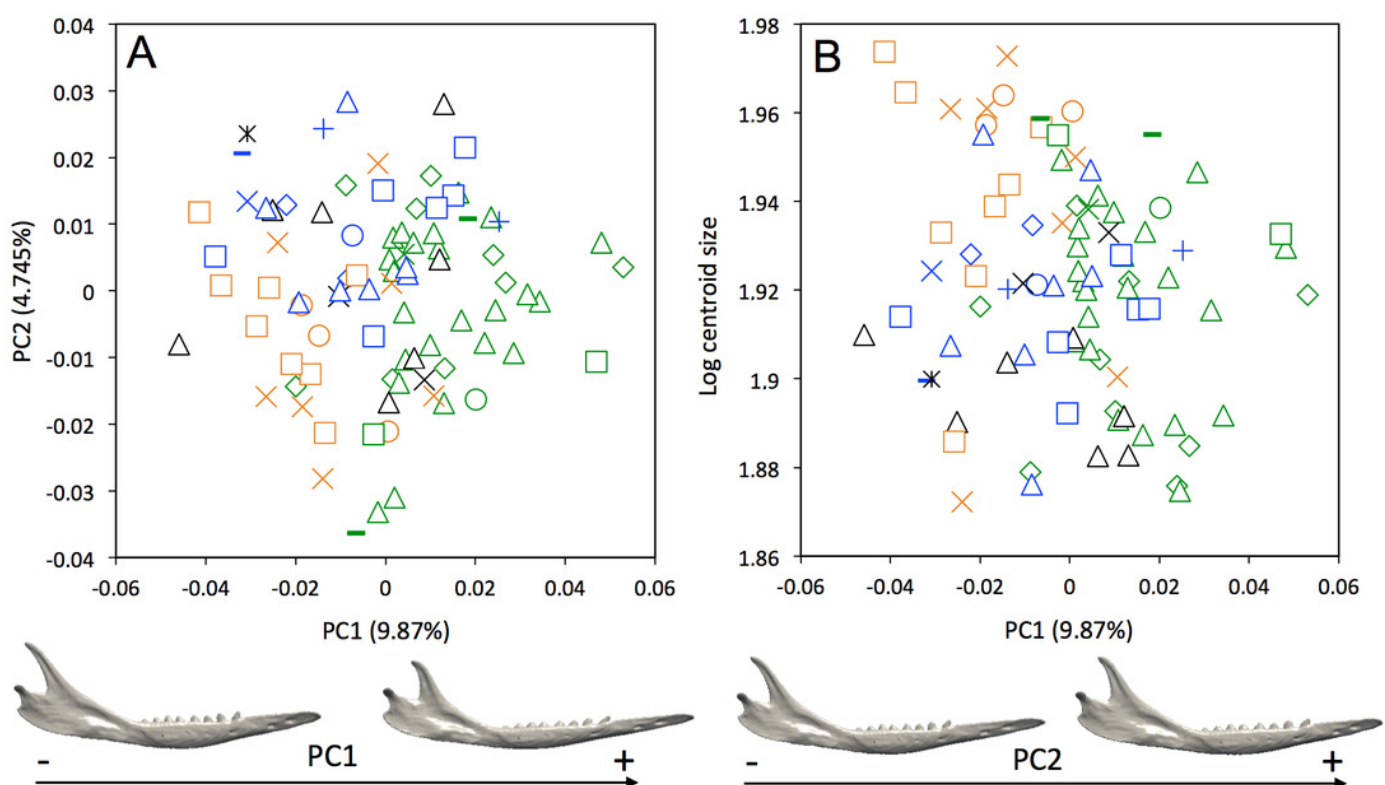
Figure 6

Figure 6

Principal component analysis (**A**, PC1 *vs* PC2; **B**, PC3 *vs* PC4) and associate patterns of morphological transformation for crania of *Dasypus novemcinctus*. *Symbols*: green diamonds, Bolivia; green triangle, Brazil (solid green triangles are for specimens from Amapa); green circles, Paraguay; green crosses, Peru; green squares, Uruguay; green bars, Venezuela; blue diamonds, Belize; blue "plus", Guatemala; blue bars, Honduras; Blue squares, Mexico; blue crosses, Nicaragua; blue triangles, USA; blue circles, Costa Rica; black triangles, Colombia; black crosses, Ecuador; orange squares, French Guiana; orange crosses, Guyana; orange circles, Suriname.
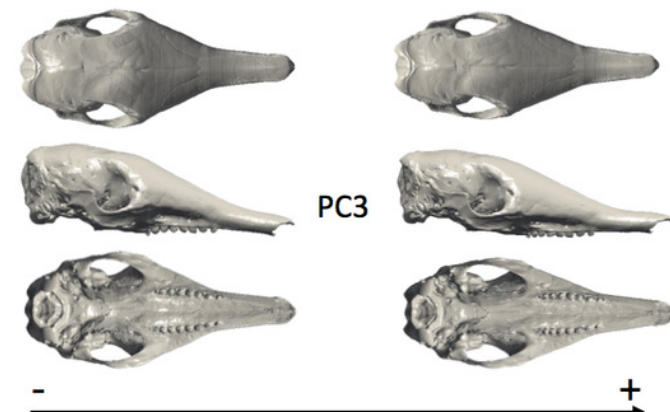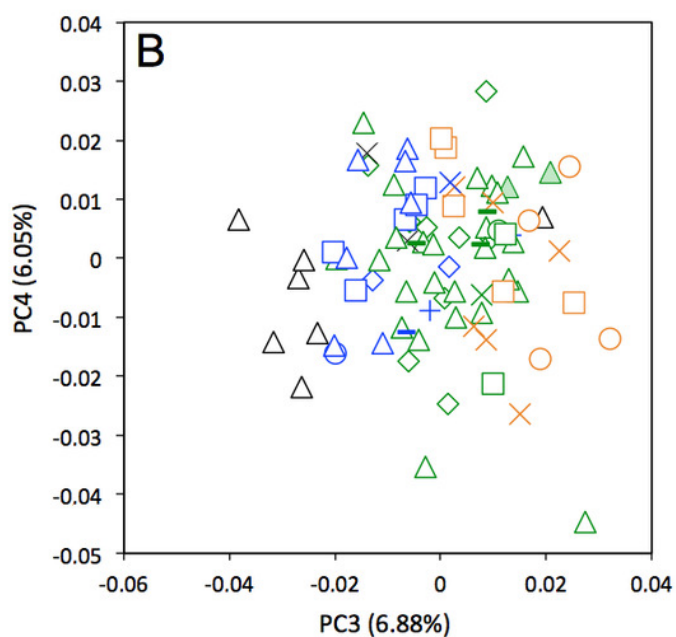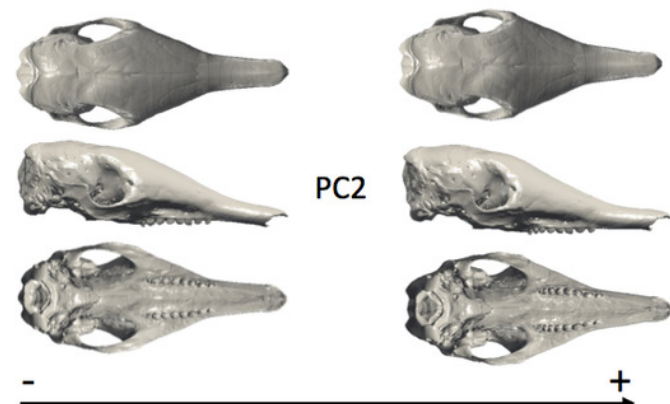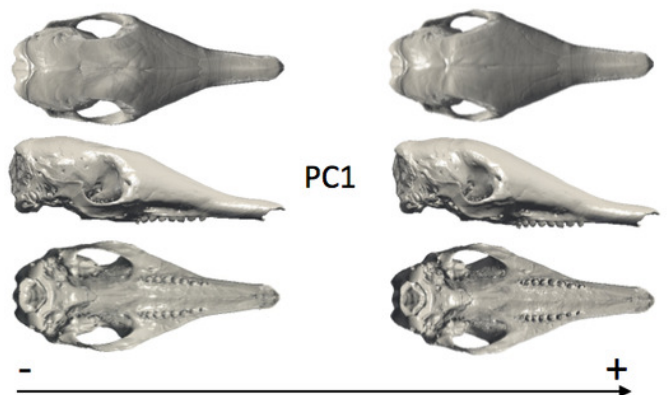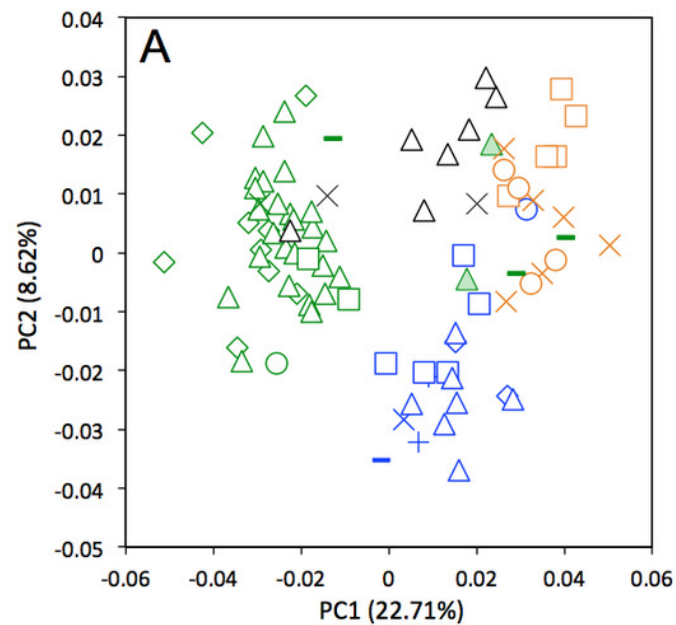
Figure 7

Figure 7

Regression of the first cranial principal component (*Dasypus novemcinctus*) on the logarithm of the centroid size (R^2=0.15; p<0.001). *Symbols*: green diamonds, Bolivia; green triangle, Brazil (solid green triangles are for specimens from Amapa); green circles, Paraguay; green crosses, Peru; green squares, Uruguay; green bars, Venezuela; blue diamonds, Belize; blue "plus", Guatemala; blue bars, Honduras; blue squares, Mexico; blue crosses, Nicaragua; blue triangles, USA; blue circles, Costa Rica; black triangles, Colombia; black crosses, Ecuador; orange squares, French Guiana; orange crosses, Guyana; orange circles, Suriname.
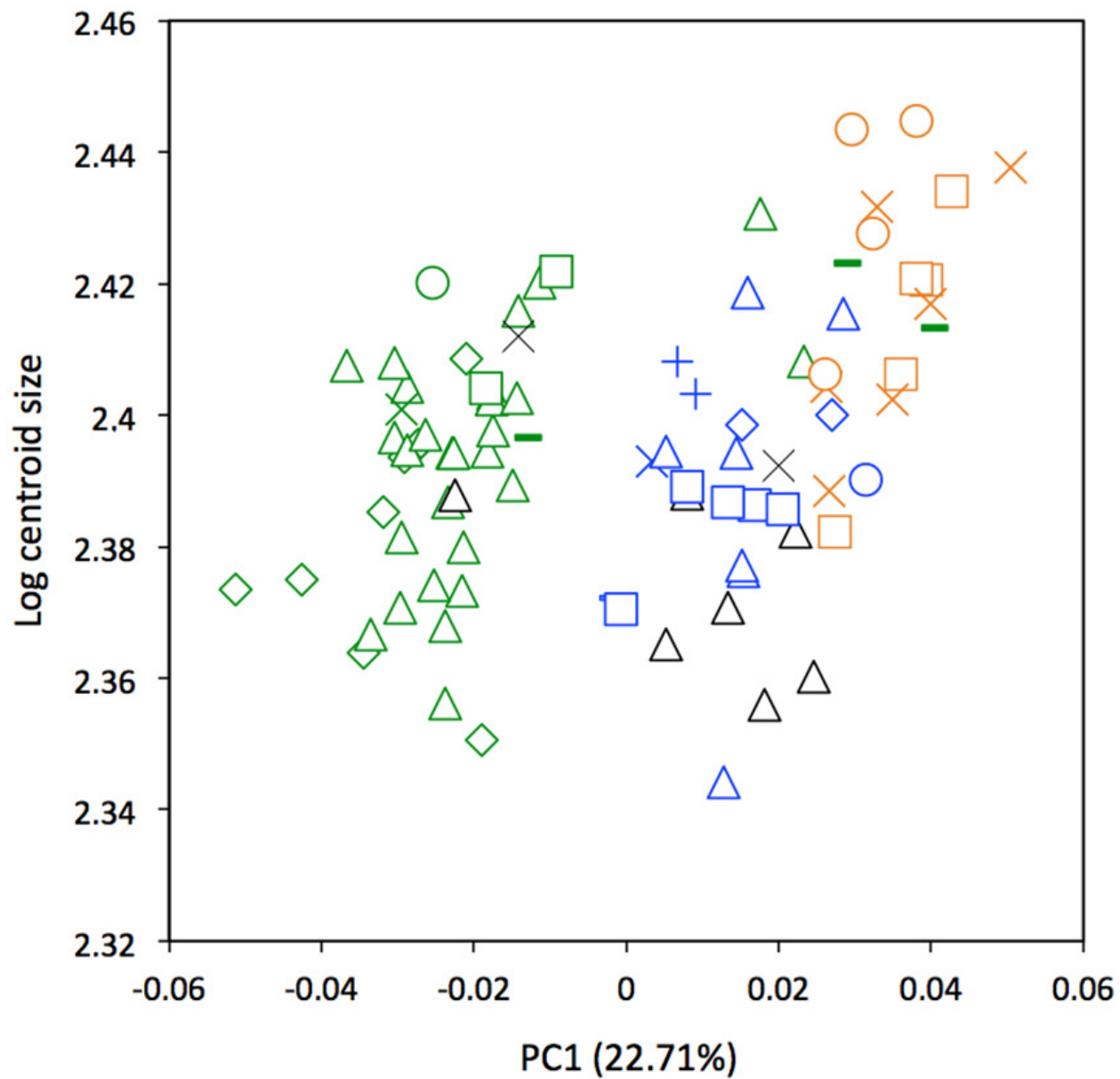
Figure 8

Figure 8

Linear Discriminant Analysis (LDA) performed on cranial shape coordinates of *Dasypus novemcinctus*. *Symbols*: green diamonds, Bolivia; green triangle, Brazil (solid green triangles are for specimens from Amapa); green circles, Paraguay; green crosses, Peru; green squares, Uruguay; green bars, Venezuela; blue diamonds, Belize; blue "plus", Guatemala; blue bars, Honduras; Blue squares, Mexico; blue crosses, Nicaragua; blue triangles, USA; black triangles, Colombia; black circles, Costa Rica; black crosses, Ecuador; orange squares, French Guiana; orange crosses, Guyana; orange circles, Suriname.
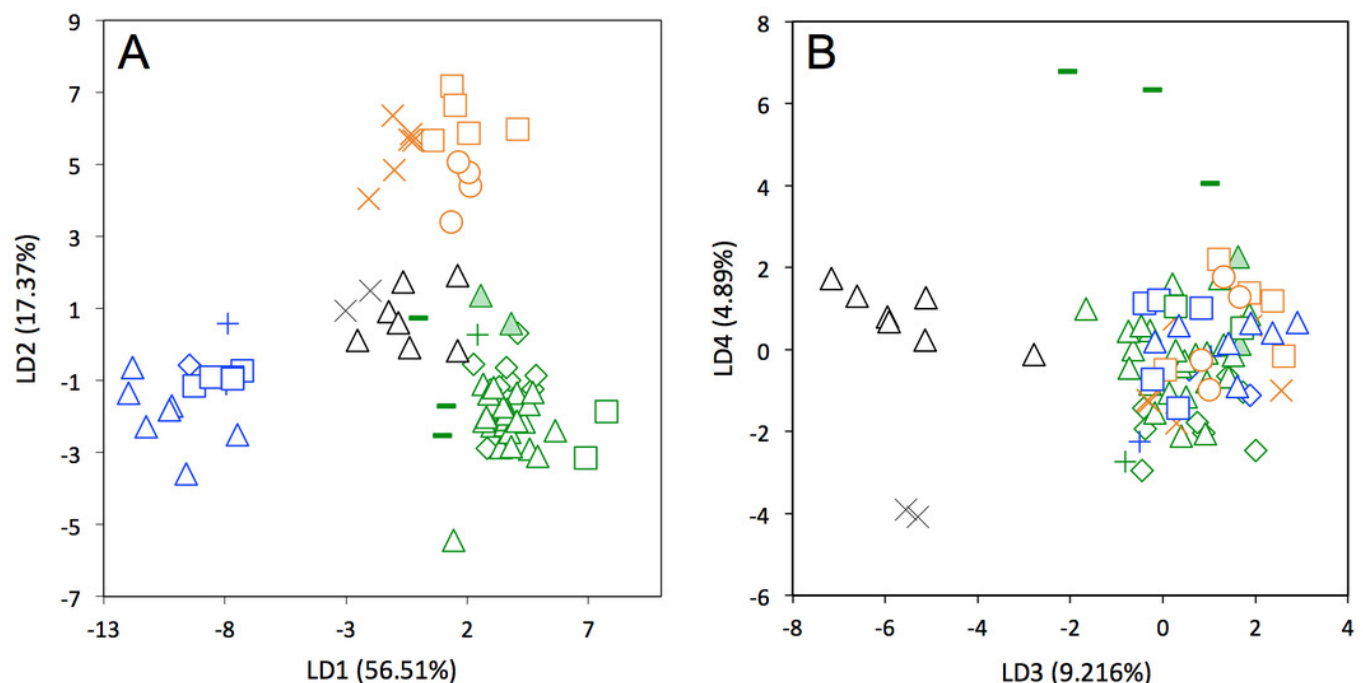
Figure 9

Figure 9

Summary map showing the geographical distribution of nine-banded armadillo specimens investigated in this study and their attribution to one of the four main morphotypes defined in this study: black, Central group; blue, Northern group; green, Southern group; orange, Guianan group. Specimens lacking precise geographical information (other than country of origin) are indicated with a square.
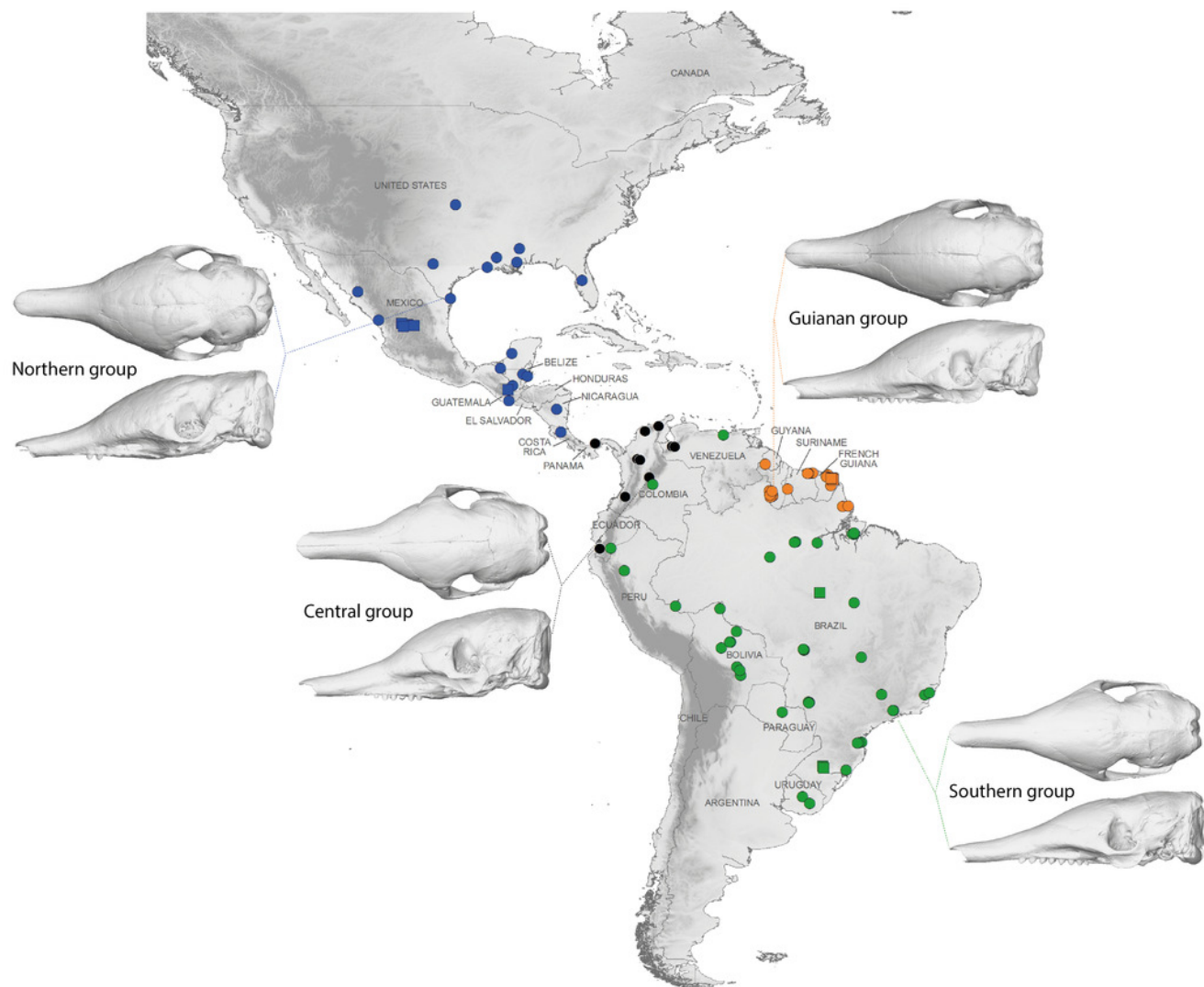
Table 1

Definitions of the landmarks used on the mandible

Numbers	Definition
1	Most anterior point of the mandible
2	Most anterior point of the alveolar margin of the tooth row
3	Most posterior point of the seventh tooth
4	Tip of the coronoid process
5	Point at the maximum of concavity between the coronoid and the condyloid processes
6	Most lateral point of the articular surface of the condyle
7	Most medial point of the articular surface of the condyle
8	Point at the maximum of concavity between the condyloid and the angular
9	Tip of the angular process
10	Mandibular foramen

Table 2

Definitions of the landmarks used on the cranium. Landmarks indicated with a star were not used in the intraspecific comparisons.

Numbers	Definition
1	Most anterodorsal point of the nasal suture
2	Intersection between inter-nasal and inter-frontal sutures
3	Intersection between inter-parietal and inter-frontal sutures
4	Intersection between inter-parietal and supra-occipal
5	Most distal point of the supra-occipal
6 and 7	Intersection between frontal, maxillar, and nasal sutures
8 and 9	Most dorsomedial point of the orbit (i.e. minimal interobital length)
10 and 11	Most posterolateral point of the supra-occipital
12 and 28	Most anterolateral point of the premaxillar/nasal suture
13 and 29	Intersection between premaxillar, maxillar, and nasal sutures
14 and 30	Interection between the lacrimal, maxillar, and frontal sutures
15 and 31	Anteroventral margin of the lacrimal foramen
16 and 32	Anteroventral margin of the upper ethmoid foramen
17 and 33	Most anterior point of the squamosal, frontal, and alisphenoid sutures
18 and 34	Most dorsal point of the maxillary foramen
19 and 35	Most dorsal point of the infraorbital foramen
20 and 36	Most anteroventral point of the sphenopalatine fissure
21 and 37	Most dorsal point of the jugal/maxillar suture
22 and 38	Most dorsal point of the jugal/squamosal suture
23 and 39	Most posterior point of the postglenoid process
24 and 40*	Most posterodorsal point of the zygomatic part of the squamosal
25 and 41	Intersection between the frontal, squamosal, and parietal sutures
26 and 42*	Most dorsal point of sulcus for external acoustic meatus on squamosal
27 and 43	Intersection between the parietal, squamosal, and supraoccipital sutures
44 and 60	Most posterior point of the premaxillar/maxillar suture in ventral view
45 and 61	Most anterior point of the alveolar margin of the premolar tooth row
46 and 62	Most posterior point of the alveolus margin of the premolar tooth row.
47 and 63	Intersection between the lacrimal/maxillar suture and the zygomasseteric crest in ventral view
48	Intersection between maxillar and palatine sutures
49 and 64	Most posterolateral point of the pterygoid wings
50 and 65	Transverse canal foramen
51 and 66	Most anterodorsal point of the *foramen ovale*
52 and 67	Most ventral of the alisphenoid/squamosal suture
53 and 68	Most lateral point between the basioccipital/basisphenoid sutures
54* and 69*	Most posterolateral point of the jugular foramen
55* and 70*	Most posterolateral point of the hypoglossal foramen
56* and 71*	Most anterolateral point of the occipital condyle
57* and 72*	Intersection between the basioccipital, the occipital condyle, and the *foramen magnum*
58*	Most antero-ventral point of the *foramen magnum*
59*	Most postero-dorsal point of the *foramen magnum*
73 and 74	Intersection between the supraoccipital, exoccipital, and petrosal sutures
75 and 76	Most posterior point of the postglenoid foramen
77 and 78	Caudal palatine foramen
79 and 80	Intersection between the lacrimal/frontal suture and the orbit
81	Most posterior point of the frontal sinuses in the midline
82	Ventral tip of the tentorial process